The Hilbert-Huang Transform in Engineering

Edited by

Norden E. Huang
Nii O. Attoh-Okine

CRC Taylor & Francis
Taylor & Francis Group

The Hilbert-Huang Transform in Engineering

The Hilbert-Huang Transform in Engineering

Edited by

Norden Huang
Nii O. Attoh-Okine

Taylor & Francis
Taylor & Francis Group

Boca Raton London New York Singapore

A CRC title, part of the Taylor & Francis imprint, a member of the
Taylor & Francis Group, the academic division of T&F Informa plc.

CRC Press
Taylor & Francis Group
6000 Broken Sound Parkway NW, Suite 300
Boca Raton, FL 33487-2742

© 2005 by Taylor & Francis Group, LLC
CRC Press is an imprint of Taylor & Francis Group, an Informa business

No claim to original U.S. Government works
Version Date: 20130925

International Standard Book Number-13: 978-1-4200-2753-2 (eBook - PDF)

This book contains information obtained from authentic and highly regarded sources. Reasonable efforts have been made to publish reliable data and information, but the author and publisher cannot assume responsibility for the validity of all materials or the consequences of their use. The authors and publishers have attempted to trace the copyright holders of all material reproduced in this publication and apologize to copyright holders if permission to publish in this form has not been obtained. If any copyright material has not been acknowledged please write and let us know so we may rectify in any future reprint.

Except as permitted under U.S. Copyright Law, no part of this book may be reprinted, reproduced, transmitted, or utilized in any form by any electronic, mechanical, or other means, now known or hereafter invented, including photocopying, microfilming, and recording, or in any information storage or retrieval system, without written permission from the publishers.

For permission to photocopy or use material electronically from this work, please access www.copyright.com (http://www.copyright.com/) or contact the Copyright Clearance Center, Inc. (CCC), 222 Rosewood Drive, Danvers, MA 01923, 978-750-8400. CCC is a not-for-profit organization that provides licenses and registration for a variety of users. For organizations that have been granted a photocopy license by the CCC, a separate system of payment has been arranged.

Trademark Notice: Product or corporate names may be trademarks or registered trademarks, and are used only for identification and explanation without intent to infringe.

Visit the Taylor & Francis Web site at
http://www.taylorandfrancis.com

and the CRC Press Web site at
http://www.crcpress.com

Published in 2005 by
CRC Press
Taylor & Francis Group
6000 Broken Sound Parkway NW, Suite 300
Boca Raton, FL 33487-2742

© 2005 by Taylor & Francis Group, LLC
CRC Press is an imprint of Taylor & Francis Group

No claim to original U.S. Government works
Printed in the United States of America on acid-free paper
10 9 8 7 6 5 4 3 2 1

International Standard Book Number-10: 0-8493-3422-5 (Hardcover)
International Standard Book Number-13: 978-0-8493-3422-1 (Hardcover)

This book contains information obtained from authentic and highly regarded sources. Reprinted material is quoted with permission, and sources are indicated. A wide variety of references are listed. Reasonable efforts have been made to publish reliable data and information, but the author and the publisher cannot assume responsibility for the validity of all materials or for the consequences of their use.

No part of this book may be reprinted, reproduced, transmitted, or utilized in any form by any electronic, mechanical, or other means, now known or hereafter invented, including photocopying, microfilming, and recording, or in any information storage or retrieval system, without written permission from the publishers.

For permission to photocopy or use material electronically from this work, please access www.copyright.com (http://www.copyright.com/) or contact the Copyright Clearance Center, Inc. (CCC) 222 Rosewood Drive, Danvers, MA 01923, 978-750-8400. CCC is a not-for-profit organization that provides licenses and registration for a variety of users. For organizations that have been granted a photocopy license by the CCC, a separate system of payment has been arranged.

Trademark Notice: Product or corporate names may be trademarks or registered trademarks, and are used only for identification and explanation without intent to infringe.

Library of Congress Cataloging-in-Publication Data

Catalog record is available from the Library of Congress

T&F informa

Taylor & Francis Group
is the Academic Division of T&F Informa plc.

Visit the Taylor & Francis Web site at
http://www.taylorandfrancis.com

and the CRC Press Web site at
http://www.crcpress.com

Preface

Data analysis serves two purposes: to determine the parameters needed to construct a model and to confirm that the model constructed actually represents the phenomenon. Unfortunately, the data — whether from physical measurements or numerical modeling — most likely will have one or more of the following problems:

- The total data are too limited.
- The data are nonstationary.
- The data represent nonlinear processes.

These problems dictate how the data can be analyzed and interpreted.

This book describes the formulation and application of the Hilbert-Huang transform (HHT) in various areas of engineering, including structural, seismic, and ocean engineering.

The primary objective of this book is to present the theory of the Hilbert-Huang Transform (HHT) and its application to engineering. The presentation of the book is such that it can be used as both a reference and a teaching text. The authors of the individual chapters provide a strong theoretical background and some new developments before addressing their specific application. This approach demonstrates the versatility of the HHT.

The book comprises 13 chapters, covering more than 300 pages. These chapters were written by 30 invited experts from 6 different countries.

The book begins with an introduction and some recent developments in HHT. Chapter 2 uses HHT to interpret nonlinear wave systems and provides a comprehensive analysis on the assessment of rogue waves. Chapter 3 discusses HHT applications in oceanography and ocean-atmosphere remote sensing data and presents some examples of these applications. Chapter 4 presents a comparison of the energy flux computation for shooting waves of HHT and wavelet analysis techniques. In Chapter 5, HHT is applied to nearshore waves, and the results are compared to field data. In Chapter 6, the author uses HHT to characterize the underwater electromagnetic environment and to identify transient manmade electromagnetic disturbances, where the HHT was able to act as a filter effectively discriminating different dipole components. Chapter 7 presents a comparative analysis of HHT and wavelet transforms applied to turbulent open channel flow data.

In Chapter 8, nonlinear soil amplification is quantified by using HHT. Chapter 9 extends the application of HHT to nonstationary random processes. Chapter 10 presents a comparative analysis of HHT wavelet and Fourier transforms in some structural health–monitoring applications. In Chapter 11, HHT is applied to molecular dynamics simulations. Chapter 12 presents a straightforward application of HHT to decomposition of wave jumps. Chapter 13, the concluding chapter, presents

perspectives on the theory and practices of HHT. It attempts to review HHT applications in biomedical engineering, chemistry and chemical engineering, financial engineering, meteorological and atmospheric studies, ocean engineering, seismic studies, structural analysis, health monitoring, and system identification. It also indicates some directions for future research.

One important feature of the book is the inclusion of a variety of modern topics. The examples presented are real-life engineering problems, as well as problems that can be useful for benchmarking new techniques.

The studies reported in this book clearly indicate an increasing interest in HHT and analysis for diversified applications. These studies are expected to stimulate the interest of other researchers around the world who are facing new challenges in new theoretical studies and innovative applications.

Norden Huang
NASA

Nii O. Attoh-Okine
University of Delaware

Acknowledgments

The editors are grateful to the contributing authors. We also wish to express our thanks to Tao Woolfe, B. J. Clark, and Michael Masiello of Taylor & Francis for providing useful feedback and guiding the editors throughout the complex editorial phase.

Norden E. Huang would like to thank Professors Theodore T. Y. Wu of the California Institute of Technology, and Owen M. Phillips of the Johns Hopkins University for their guidance and encouragement throughout the years, without which the Hilbert-Huang Transform would not be what it is today.

Nii O. Attoh-Okine, the co-editor of the book, wishes to express his gratitude to his parents, Madam Charkor Quaynor, and Richard Attoh-Okine, for their support and encouragement through the years.

Contributors

Nii O. Attoh-Okine
Civil Engineering Department
University of Delaware
Newark, Delaware

Brad Battista
Information Systems Laboratories, Inc.
San Diego, California

Rodney R. Buntzen
Information Systems Laboratories, Inc.
San Diego, California

Marcus Dätig
Civil Engineering Department
Bergische University Wuppertal
Wuppertal, Germany

Brian Dzwonkowski
Graduate College of Marine Studies
University of Delaware
Newark, Delaware

Colin M. Edge
GlaxoSmithKline Pharmaceuticals
Harlow, United Kingdom

Jonathan W. Essex
School of Chemistry
University of Southampton
Southampton, United Kingdom

Michael Gabbay
Information Systems Laboratories, Inc.
San Diego, California

Robert J. Gledhill
School of Chemistry
University of Southampton
Southampton, United Kingdom

Ping Gu
Department of Civil Engineering
University of Illinois at Urbana-Champaign
Urbana, Illinois

Norden E. Huang
Goddard Institute for Data Analysis
NASA Goddard Space Flight Center
Greenbelt, Maryland

Paul A. Hwang
Oceanography Division
Naval Research Laboratory
Stennis Space Center, Mississippi

Lide Jiang
Graduate College of Marine Studies
University of Delaware
Newark, Delaware

Young-Heon Jo
Graduate College of Marine Studies
University of Delaware
Newark, Delaware

James M. Kaihatu
Oceanography Division
Naval Research Laboratory
Stennis Space Center, Mississippi

Michael L. Larsen
Information Systems Laboratories, Inc.
San Diego, California

Stephen C. Phillips
School of Chemistry
University of Southampton
Southampton, United Kingdom

Panayotis Prinos
Department of Civil Engineering
Aristotle University of Thessaloniki
Thessaloniki, Greece

Ser-Tong Quek
Department of Civil Engineering
National University of Singapore
Singapore

Jeffrey Ridgway
Information Systems Laboratories, Inc.
San Diego, California

Torsten Schlurmann
Civil Engineering Department
Bergische University Wuppertal
Wuppertal, Germany

Martin T. Swain
School of Chemistry
University of Southampton
Southampton, United Kingdom

Puat-Siong Tua
Department of Civil Engineering
National University of Singapore
Singapore

Albena Dimitrova Veltcheva
Port and Airport Research Institute
Yokosuka, Japan

Cye H. Waldman
Information Systems Laboratories, Inc.
San Diego, California

David W. Wang
Oceanography Division
Naval Research Laboratory
Stennis Space Center, Mississippi

Quan Wang
Department of Civil Engineering
National University of Singapore
Singapore

Wei Wang
Physical Oceanography Laboratory
Ocean University of China
Shandong, P. R. China

Yi-Kwei Wen
Department of Civil Engineering
University of Illinois at Urbana-Champaign
Urbana, Illinois

Adrian P. Wiley
School of Chemistry
University of Southampton
Southampton, United Kingdom

Xiao-Hai Yan
Graduate College of Marine Studies
University of Delaware
Newark, Delaware

Athanasios Zeris
Department of Civil Engineering
Aristotle University of Thessaloniki
Thessaloniki, Greece

Ray Ruichong Zhang
Division of Engineering
Colorado School of Mines
Golden, Colorado

Contents

1 Introduction to Hilbert-Huang Transform and Some Recent Developments

Norden E. Huang

CONTENTS

1.1 INTRODUCTION

Hilbert-Huang transform (HHT) is the designated name for the result of empirical mode decomposition (EMD) and the Hilbert spectral analysis (HSA) methods, which were both introduced recently by Huang et al. (1996, 1998, 1999, and 2003), specifically for analyzing data from nonlinear and nonstationary processes. Data analysis is an indispensable step in understanding the physical processes, but traditionally the data analysis methods were dominated by Fourier-based analysis. The problems of such an approach were discussed in detail by Huang et al. (1998). As data analysis is important for both theoretical and experimental studies (for data is the only real link between theory and reality), we desperately need new methods in order to gain a deeper insight into the underlying processes that actually generate the data. The method we really need should not be limited to linear and stationary processes, and it should yield physically meaningful results.

The development of the HHT is motivated precisely by such needs: first, because the natural physical processes are mostly nonlinear and nonstationary, there are very limited options in data analysis methods that can correctly handle data from such processes. The available methods are either for linear but nonstationary processes (such as the wavelet analysis, Wagner-Ville, and various short-time Fourier spectrograms as summarized by Priestley [1988], Cohen [1995], Daubechies [1992], and Flandrin [1999]) or for nonlinear but stationary and statistically deterministic processes (such as the various phase plane representations and time-delayed imbedded methods as summarized by Tong [1990], Diks [1997], and Kantz and Schreiber [1997]). To examine data from real-world nonlinear, nonstationary, and stochastic processes, we urgently need new approaches.

Second, the nonlinear processes need special treatment. Other than periodicity, we want to learn the detailed dynamics in the processes from the data. One of the typical characteristics of nonlinear processes, proposed by Huang et al. (1998), is the intra-wave frequency modulation, which indicates that the instantaneous frequency changes within one oscillation cycle. Let us examine a very simple nonlinear system given by the nondissipative Duffing equation as

$$\frac{\partial^2 x}{\partial t^2} + x + \varepsilon x^3 = \gamma \cos \omega t \ , \tag{1.1}$$

where ε is a parameter not necessarily small and γ is the amplitude of a periodic forcing function with a frequency ω.

In Equation 1.1, if the parameter ε were zero, the system is linear, and the solution would be easy. For a small, however, the system is nonlinear, but it could be solved easily with perturbation methods. If ε is not small compared to unity, then the system is highly nonlinear. No known general analytic method is available for this condition; we have to resort to numerical solutions, where all kinds of complications such as bifurcations and chaos can result.

Even with these complications, let us examine the qualitative nature of the solution for Equation 1.1 by rewriting it in a slightly different way, as

$$\frac{\partial^2 x}{\partial t^2} + x(1 + \varepsilon x^2) = \gamma \cos \omega t \ , \tag{1.2}$$

where the symbols are defined as in Equation 1.1. Then the quantity within the parentheses can be regarded as a variable spring constant or a variable pendulum length. With this view, we can see that the frequency should be changing from location to location and from time to time, even within one oscillation cycle.

As Huang et al. (1998) pointed out, this intra-frequency frequency variation is the hallmark of nonlinear systems. In the past, there has been no clear way to depict this intra-wave frequency variation by using Fourier-based analysis methods, except to resort to the harmonics. Even by the classical Hamiltonian approach, in which the frequency is defined as the rate of change of the Hamiltonian with respect to

the action, we still cannot gain any more insight, for the definition of the action is an integration of generalized momentum along the generalized coordinates; therefore, there is no instantaneous value. Thus, the best we could do for any nonlinear distorted waveform in the earlier approaches was to refer to harmonic distortions. Harmonic distortion is, in fact, a rather poor alternative, for it is the result obtained by imposing a linear structure on a nonlinear system. Consequently, the results may make perfect mathematical sense, but at the same time they have absolutely no physical meaning. The physically meaningful way to describe the system should be in terms of the instantaneous frequency.

The easiest way to compute the instantaneous frequency is by the Hilbert transform, through which we can find the complex conjugate, $y(t)$, of any real valued function $x(t)$ of L^p class,

$$y(t) = \frac{1}{\pi} P \int_{-\infty}^{\infty} \frac{x(\tau)}{t-\tau} d\tau \,, \tag{1.3}$$

in which the P indicates the principal value of the singular integral. With the Hilbert transform, we have

$$z(t) = x(t) + j\, y(t) = a(t) e^{j\theta(t)} \,, \tag{1.4}$$

where

$$a(t) = \left(x^2 + y^2\right)^{1/2} \quad ; \quad \theta(t) = \tan^{-1} \frac{y}{x} \,. \tag{1.5}$$

Here a is the instantaneous amplitude and θ is the phase function; thus the instantaneous frequency is simply

$$\omega = -\frac{d\theta}{dt} \,. \tag{1.6}$$

As the instantaneous frequency is defined through a derivative, it is very local and can be used to describe the detailed variation of frequency, including the intra-wave frequency variation. As simple as this principle is, the implementation is not at all trivial. To represent the function in terms of a meaningful amplitude and phase, however, requires that the function satisfy certain conditions. Let us take the length-of-day (LOD) data, given in Figure 1.1, as an example to explain this requirement. The daily data covers from 1962 to 2002, for roughly 40 years. After performing the Hilbert transform, the polar representation of the data is given in Figure 1.2, which is a random collection of intertwined looping curves. The corresponding phase function is given in Figure 1.3, where random finite jumps intersperse within

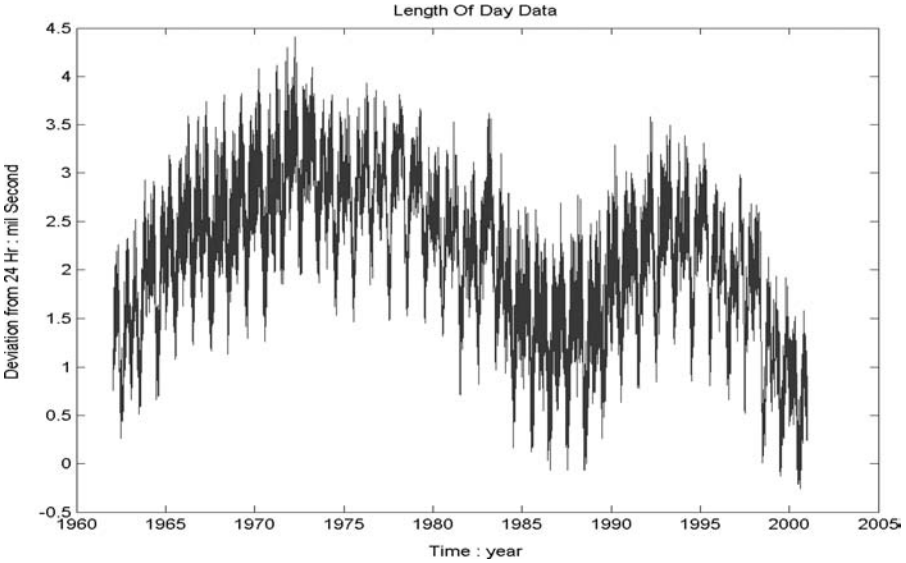

FIGURE 1.1 (See color insert following page 20). Data of Length-of-Day measure the deviation from the mean 24-hour-day.

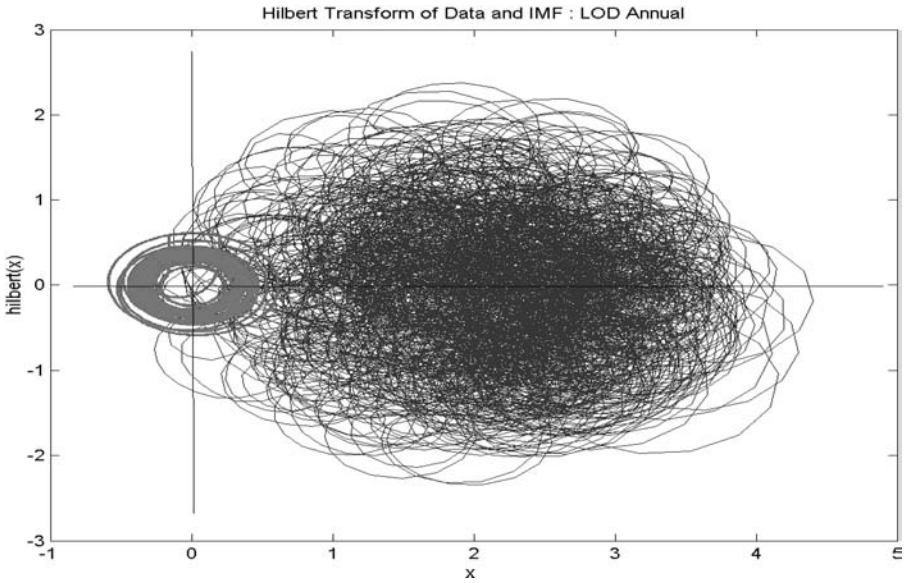

FIGURE 1.2 (See color insert following page 20). Analytic function in complex phase plane formed by the real data and it Hilbert Transform. It shows not apparent order. After the EMD, the annual cycle is extract and plotted also.

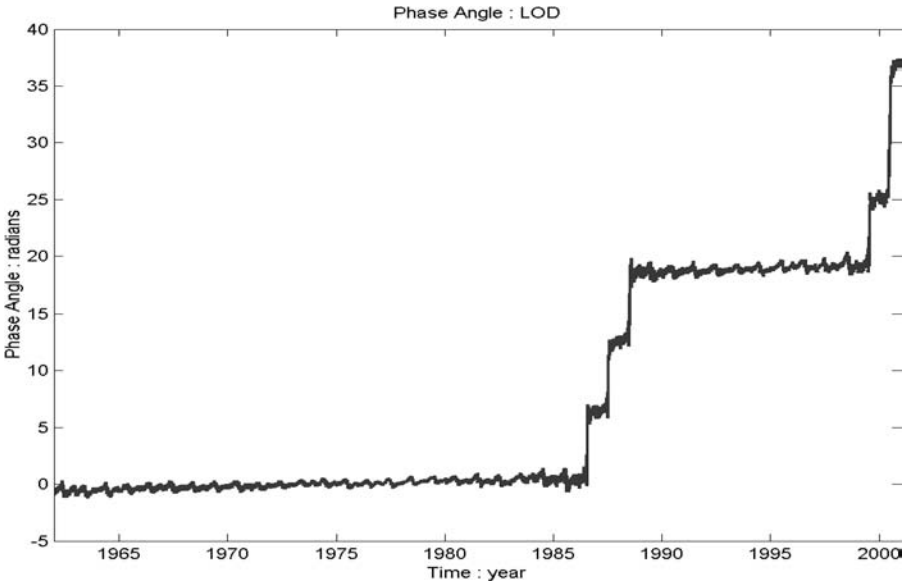

FIGURE 1.3 The phase function of the analytic function based on the Length-of-Day data.

the data span. If we follow through the definition of the instantaneous frequency as given in Equation 1.6 literally, we would have a totally nonsensical result, as given in Figure 1.4, where the instantaneous frequency is equally likely to be positive or negative. Unfortunately, this is exactly the procedure recommended by Hahn (1996).

To show how this should not be the case, let us consider the three curves given by the following three expressions

$$\begin{aligned} x_1 &= \sin \omega t \; ; \\ x_2 &= 0.5 + \sin \omega t \; ; \\ x_3 &= 1.5 + \sin \omega t \; ; \end{aligned} \tag{1.7}$$

shown in Figure 1.5. All three curves are perfect sine functions, but with the mean displaced: for x_1, its mean is exactly zero; for x_2, its mean is moved up by half of its amplitude; for x_3, its mean is moved up by 1.5 times its amplitude. As a result, the curve represented by x_3 is totally above the zero reference axis. If we perform the Hilbert transform to all three functions given in Equation 1.7, we would get three different circles in the phase plane, with the centers of two of the circles displaced by the amount of the added constants, as shown in Figure 1.6. Consequently, the phase functions from the three circles will be different, as shown in Figure 1.7: for x_1, the phase function is a straight line; for x_2, the phase function is a wavy line, but the general trend still agrees with the straight line; for x_3, the phase function is also wavy, but the variation is always within $\pm \pi$.

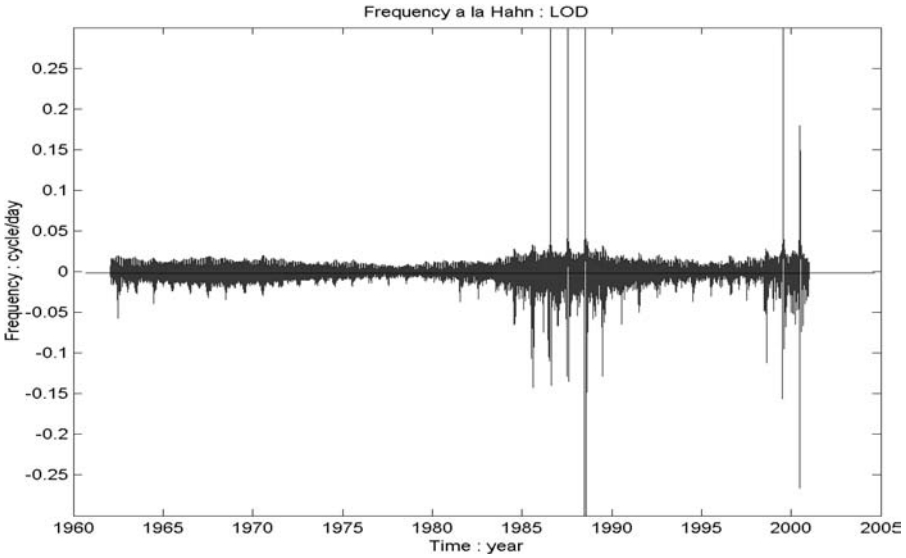

FIGURE 1.4 Instantaneous frequency obtained form derivative of the phase function without decomposition first. The values are equally like to be positive as negative.

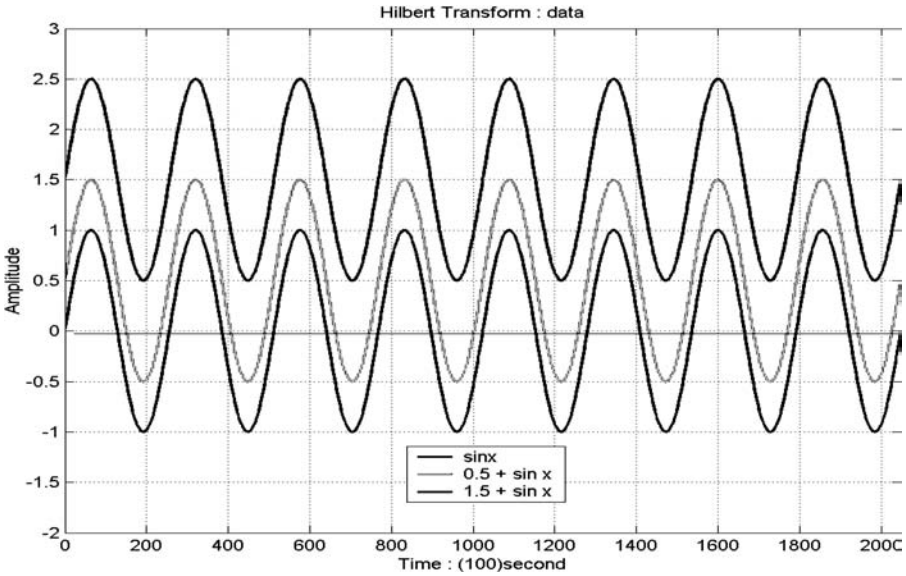

FIGURE 1.5 (See color insert following page 20). Model data to illustrate the fallacy of the instantaneous frequency without decomposition.

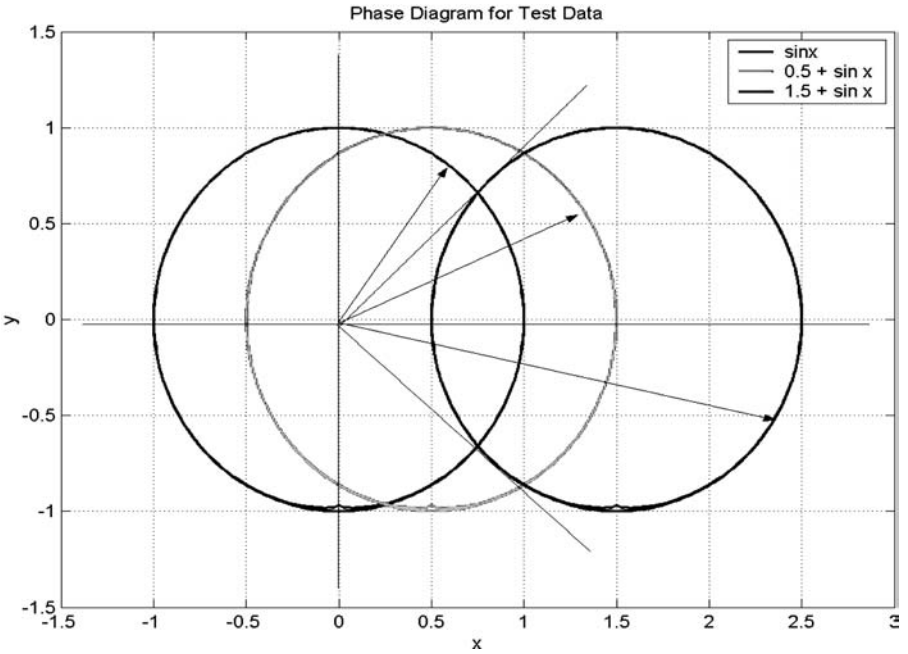

FIGURE 1.6 (See color insert following page 20). The analytic function in complex phase plane of the data given in Figure 1.5.

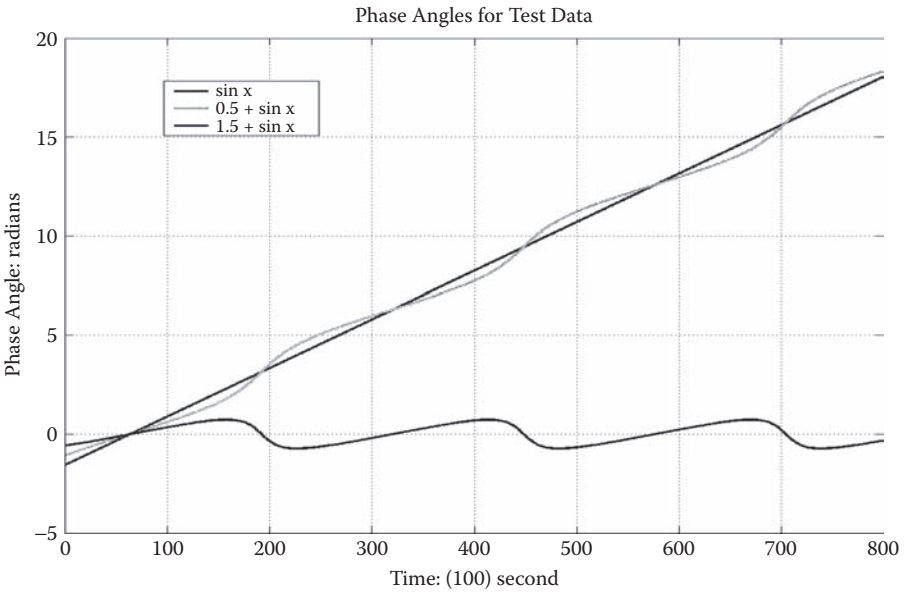

FIGURE 1.7 (See color insert following page 20). Phase function of the model function given in Figure 1.5.

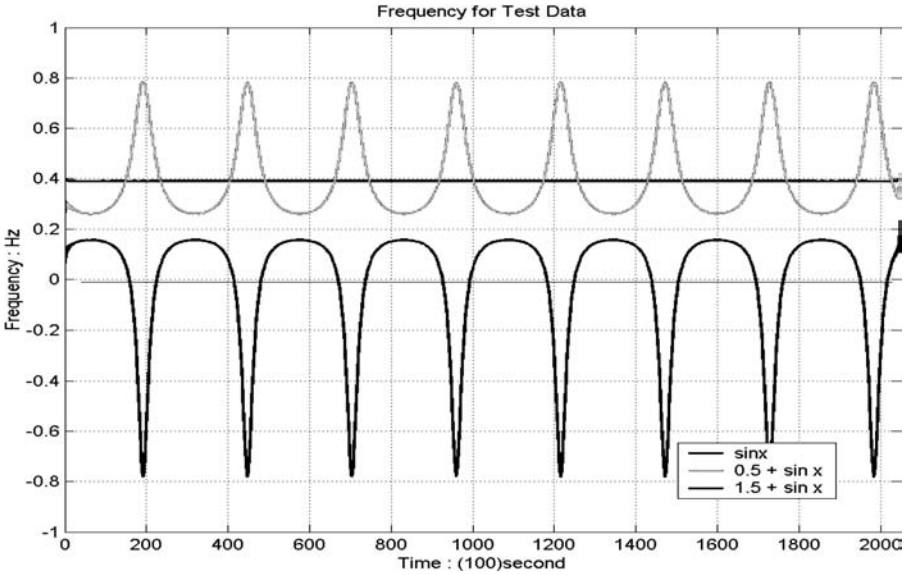

FIGURE 1.8 (See color insert following page 20). Instantaneous frequency computed from the cosine model functions consist of the identical cosine function with different displacements.

Based on these phase functions, the instantaneous frequency values are very different for the three expressions, as shown in Figure 1.8: for x_1, the instantaneous frequency is a constant value, which is exactly what we expected; for x_2, the instantaneous frequency is a variable curve with all positive values; for x_3, the instantaneous frequency is a highly variable curve fluctuating from positive to negative values. Even if we are prepared to accept negative frequency, the result of three different values for the same sine wave with only a displaced mean is very unsettling: some of the results are, of course, nonsensical. The only meaningful result is from the sine curve with a zero mean.

What went wrong was the fact that two of the curves do not have a zero mean, or the envelopes of the curves are not symmetric with respect to the zero axis. Thus, before performing the Hilbert transform, we have to preprocess the data. In the past, any preprocessing usually consisted of band-pass filtering. For some of the data from linear and stationary processes, this band-pass filtering method will give the correct results. For data from nonlinear and nonstationary processes, however, the band-pass filter will alter the characteristics of the filtered curve. The problem with the filtering approach is that all the frequency domain filters are Fourier-based, which means they are established under linear and stationary assumptions. When the data are from nonlinear and nonstationary processes, such Fourier-based analysis will surely generate spurious harmonics, which are mathematically necessary but physically meaningless, as discussed by Huang et al. (1998, 1999).

Considering these points leads us to this conclusion: *The correct preprocessing for data from nonlinear and nonstationary processes will have to be adaptive and*

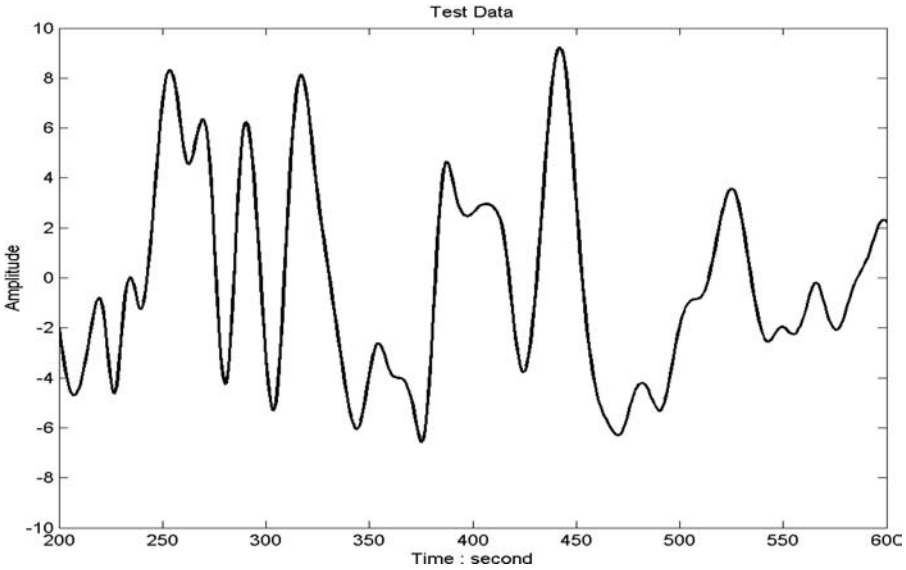

FIGURE 1.9 Test data to illustrate the procedures of Empirical Mode Decomposition also known as sifting.

implemented in the time domain. The only method presently known to achieve this is based on the Hilbert-Huang transform proposed by Huang et al. (1996, 1998, 1999, and 2003). This method is the subject of the next section.

1.2 THE HILBERT-HUANG TRANSFORM

The Hilbert-Huang transform is the result of the empirical mode decomposition and the Hilbert spectral analysis. As the EMD method is more fundamental, and it is a necessary step to reduce any given data into a collection of intrinsic mode functions (IMF) to which the Hilbert analysis can be applied (see, for example, Huang et al., 1996, 1998, and 1999), we will discuss it first. An IMF represents a simple oscillatory mode as a counterpart to the simple harmonic function, but it is much more general: by definition, an IMF is any function with the same number of extrema and zero crossings, with its envelopes, as defined by all the local maxima and minima, being symmetric with respect to zero. Obtaining the EMD consists of the following steps:

For any data as given in Figure 1.9, we first identify all the local extrema and then connect all the local maxima by a cubic spline line as the upper envelope. We repeat the procedure for the local minima to produce the lower envelope. The upper and lower envelopes should cover all the data between them. Their mean is designated as m_1, as shown in Figure 1.10, and the difference between the data and m_1 is the first proto-IMF (PIMF) component, h_1:

$$x(t) - m_1 = h_1 \ . \tag{1.8}$$

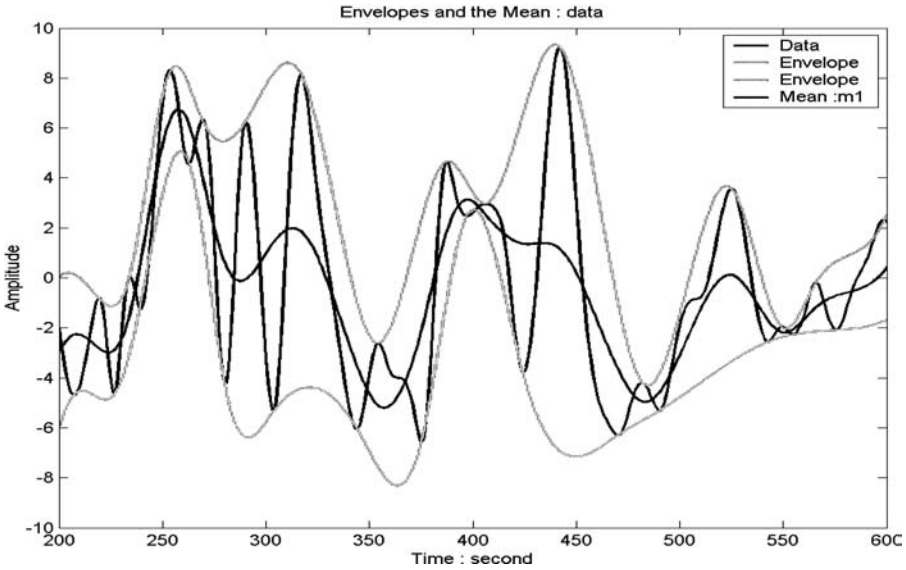

FIGURE 1.10 (See color insert following page 20). The cubic spline upper and the lower envelopes and their mean, $\boldsymbol{m_1}$.

This result is shown in Figure 1.11. The procedure of extracting an IMF is called *sifting*. By construction, this PIMF, h_1, should satisfy the definition of an IMF, but the change of its reference frame from rectangular coordinate to a curvilinear one can cause anomalies, as shown in Figure 1.11, where multi-extrema between successive zero-crossings still existed. To eliminate such anomalies, the sifting process has to be repeated as many times as necessary to eliminate all the riding waves. In the subsequent sifting process steps, h_1 is treated as the data. Then

$$h_1 - m_{11} = h_{11}, \tag{1.9}$$

where m_{11} is the mean of the upper and lower envelopes of h_1. This process can be repeated up to k times; then, h_{1k} is given by

$$h_{1(k-1)} - m_{1k} = h_{1k}. \tag{1.10}$$

Each time the procedure is repeated, the mean moves closer to zero, as shown in Figures 1.12a, b, and c. Theoretically, this step can go on for many iterations, but each time, as the effects of the iterations make the mean approach zero, they also make amplitude variations of the individual waves more even. Yet the variation of the amplitude should represent the physical meaning of the processes. Thus this iteration procedure, though serving the useful purpose of making the mean to be zero, also drains the physical meaning out of the resulting components if carried too far. Theoretically, if one insists on achieving a strictly zero mean, one would

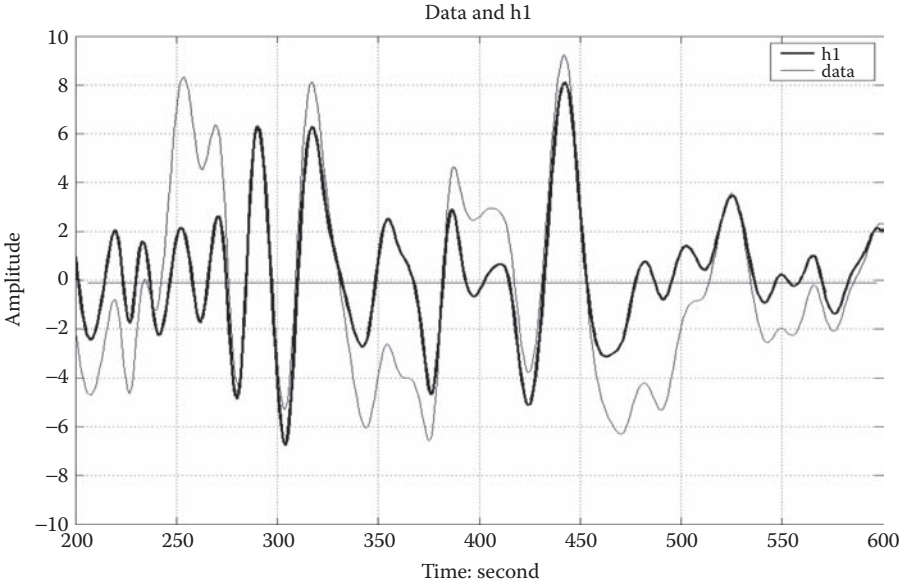

FIGURE 1.11 (See color insert following page 20). Comparison between data and h_1, as given by Equation (1.9). Note most, but not all, riding waves are eliminated in h_1.

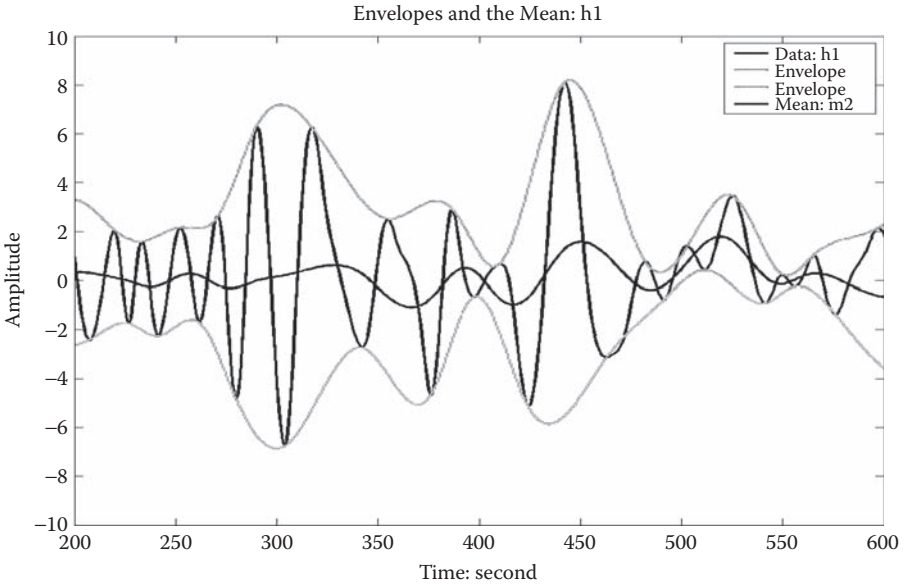

FIGURE 1.12 (A) (See color insert following page 20). Repeat the sifting using h_1 as data.

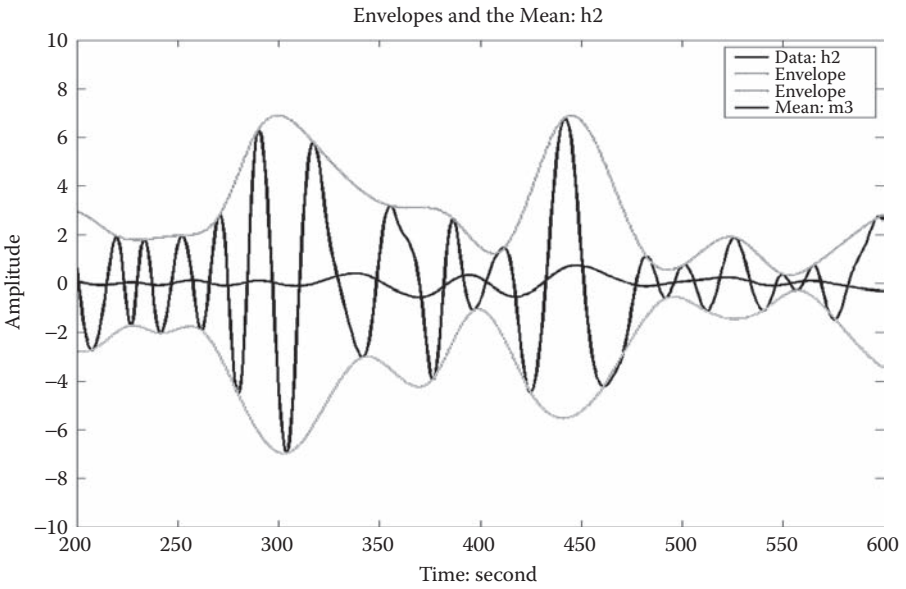

FIGURE 1.12 (B) (See color insert following page 20). Repeat the sifting using h_2 as data.

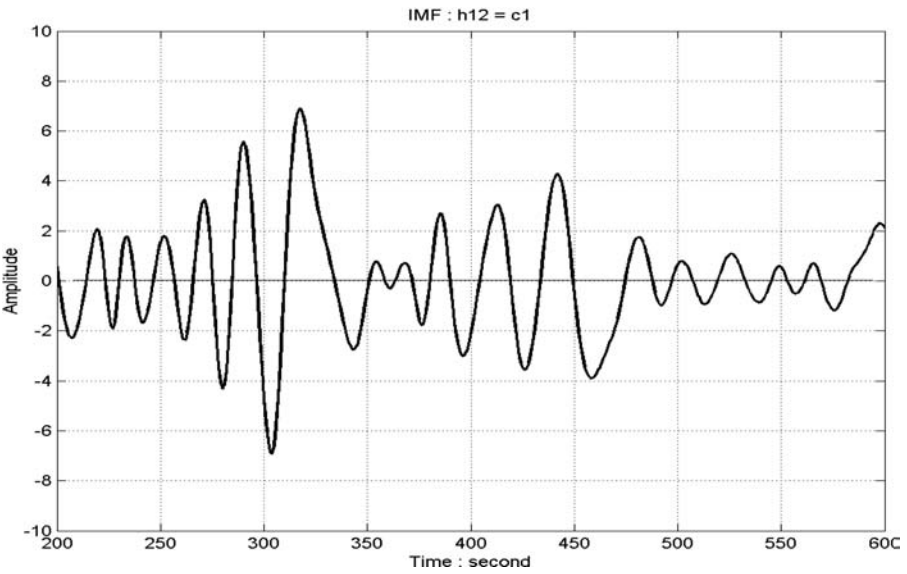

FIGURE 1.12 (C) (See color insert following page 20). After 12 iterations, the first Intrinsic Mode Function is found.

probably have to make the resulting components purely frequency-modulated functions, with the amplitude becoming constant. Then the resulting component would not retain any physically meaningful information. Thus to attain the delicate balance of achieving a reasonably small mean and also retaining enough physical meaning in the resulting component, we have proposed two stoppage criteria. The "stoppage criterion" actually determines the number of sifting steps to produce an IMF; it is thus of critical importance in a successful implementation of the EMD method.

The first stoppage criterion is similar to the Cauchy convergence test, where we first define a sum of the difference, SD, as

$$SD = \frac{\sum_{t=0}^{T} \left| h_{k-1}(t) - h_k(t) \right|^2}{\sum_{t=0}^{T} h_{k-1}^2(t)}; \tag{1.11}$$

then the sifting will stop when SD is smaller than a preassigned value. This definition is a slight modification from the original one proposed by Huang et al. (1998), where the SD was defined simply as

$$SD = \sum_{t=0}^{T} \frac{\left| h_{k-1}(t) - h_k(t) \right|^2}{h_{k-1}^2(t)}. \tag{1.12}$$

The shortcoming of this old definition as given in Equation 1.12 is that the value of SD can be dominated by local small values of h_{k-1}, while the definition given in Equation 1.11 sums up all the contributions over the whole duration of the data. Even with this modification, there is still a problem with this seemingly mathematically sound approach: in this definition, the important criterion that the number of extrema has to equal the number of zero-crossings has not been checked. To overcome this practical difficulty, Huang et al. (1999, 2003) proposed an alternative in a second stoppage criterion.

The second stoppage criterion is based on a number called the S-number, which is defined as the number of consecutive siftings when the numbers of zero-crossings and extrema are equal or at most differing by one; it requires that number shall remain unchanged. Through exhaustive testing, Huang et al. (2003) used this S-number method of defining a stoppage criterion to establish a confidence limit for the EMD, to be discussed later.

When the resulting function satisfies either of the criteria given above, this component is designated as the first IMF, c_1, as shown in Figure 1.12c. We can then separate c_1 from the rest of the data by

$$X(t) - c_1 = r_1. \tag{1.13}$$

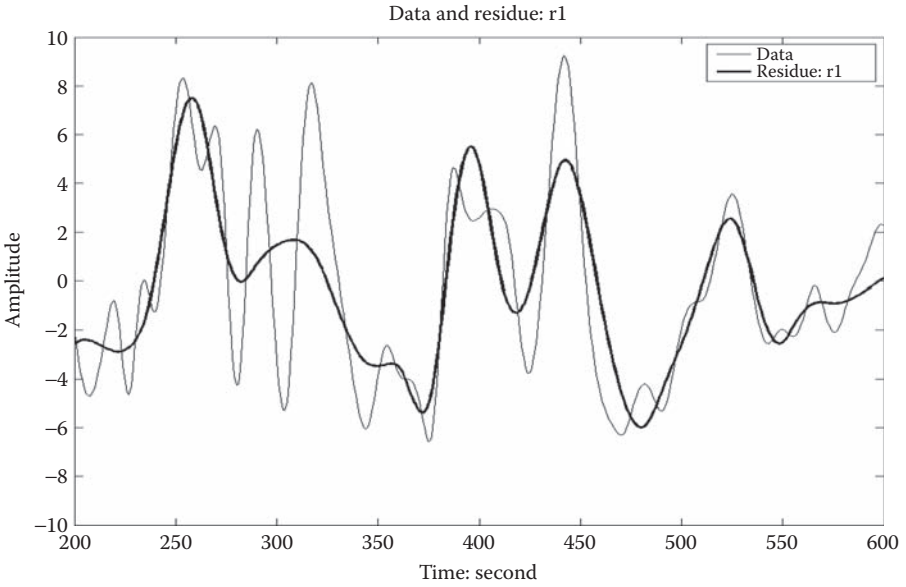

FIGURE 1.13 (See color insert following page 20). Comparison between data and the residue, r_1, after the first IMF, c_1, is removed. Notice the residue behaves like a moving mean to the data that bisect all the waves.

This resulting residue is shown in Figure 1.13. Since the residue, r_1, still contains information with longer periods, it is treated as the new data and subjected to the same process as described above. This procedure can be repeated to all the subsequent r_j's, and the result is

$$\begin{aligned} r_1 - c_2 &= r_2, \\ &\ldots \\ r_{n-1} - c_n &= r_n \end{aligned} \qquad (1.14)$$

By summing up Equation 1.13 and Equation 1.14, we finally obtain

$$X(t) = \sum_{j=1}^{n} c_j + r_n . \qquad (1.15)$$

Thus, we achieve a decomposition of the data into n IMF modes, and a residue, r_n, which can be either a constant, a monotonic mean trend, or a curve having only one extremum. Recent studies by Flandrin et al. (2004) and Wu and Huang (2004) established that the EMD is a dyadic filter, and it is equivalent to an adaptive wavelet. Since it is adaptive, we avoid the shortcomings of using an *a priori*–defined wavelet basis, and we also avoid the spurious harmonics that would have resulted. The

components of the EMD are usually physically meaningful, for the characteristic scales are defined by the physical data. The sifting process is, in fact, a Reynolds-type decomposition: separating variations from the mean, except that the mean is a local instantaneous mean, so that the different modes are almost orthogonal to each other, except for the nonlinearity in the data.

Having obtained the intrinsic mode function components, we can apply the Hilbert transform to each IMF component and compute the instantaneous frequency as the derivative of the phase function. After performing the Hilbert transform to each IMF component, we can express the original data as the real part, *RP*, in the following form:

$$X(t) = RP \sum_{j=1}^{n} a_j(t) e^{i\int \omega_j(t)dt} \tag{1.16}$$

Equation 1.16 gives both amplitude and frequency of each component as a function of time. The same data, if expanded in a Fourier representation, would have a constant amplitude and frequency for each component. The contrast between EMD and Fourier decomposition is clear: the IMF represents a generalized Fourier expansion with a time-varying function for amplitude and frequency. This frequency–time distribution of the amplitude is designated as the Hilbert amplitude spectrum, *H(, t)*, or simply the Hilbert spectrum.

With the Hilbert spectrum defined, we can also define the marginal spectrum, *h()*, as

$$h(\omega) = \int_0^T H(\omega, t)dt. \tag{1.17}$$

The marginal spectrum offers a measure of total amplitude (or energy) contribution from each frequency value. It represents the cumulated amplitude over the entire data span in a probabilistic sense.

The combination of the EMD and the HSA is known as the Hilbert-Huang transform for short. Empirically, all tests indicate that HHT is a superior tool for time–frequency analysis of nonlinear and nonstationary data. It has an adaptive basis, and the frequency is defined through the Hilbert transform. Consequently, there is no need for the spurious harmonics to represent nonlinear waveform deformations as in any of the *a priori* basis methods, and there is no uncertainty principle limitation on time or frequency resolution resulting from the convolution pairs possessing *a priori* bases. Table 1.1 compares Fourier, wavelet, and HHT analyses.

From this table, we can see that the HHT approach is indeed a powerful method for the analysis of data from nonlinear and nonstationary processes: it has an adaptive basis; the frequency is derived by differentiation rather than convolution — therefore, it is not limited by the uncertainty principle; it is applicable to nonlinear and nonstationary data; and it presents the results in time–frequency–energy space for feature extraction. This basic development of the HHT method has been followed

TABLE 1.1
Comparisons between Fourier, Wavelet, and Hilbert-Huang Transform in Data Analysis

	Fourier	Wavelet	Hilbert
Basis	A priori	A priori	Adaptive
Frequency	Convolution: global, uncertainty	Convolution: regional, uncertainty	Differentiation: local, certainty
Presentation	Energy–frequency	Energy–time–frequency	Energy–time–frequency
Nonlinear	No	No	Yes
Nonstationary	No	Yes	Yes
Feature Extraction	No	Discrete: no Continuous: yes	Yes
Theoretical Base	Theory complete	Theory complete	Empirical

by recent developments that have either added insight to the results or enhanced their statistical significance. Some of the recent developments are summarized in the following section.

1.3 THE RECENT DEVELOPMENTS

We will discuss in some detail recent developments in the areas of the normalized Hilbert transform, the confidence limit, and the statistical significance of IMFs.

1.3.1 The Normalized Hilbert Transform

It is well known that, although the Hilbert transform exists for any function of L^p class, the phase function of the transformed function will not always yield physically meaningful instantaneous frequencies, as discussed above. In addition to the requirement of being an IMF, which is only a necessary condition, additional limitations have been summarized succinctly in two theorems.

First, the Bedrosian theorem (1963) states that the Hilbert transform for the product of two functions, *f(t)* and *h(t)*, can be written as

$$H[f(t)h(t)] = f(t)H[h(t)], \tag{1.18}$$

only if the Fourier spectra for *f(t)* and *h(t)* are totally disjoint in frequency space, and if the frequency content of the spectrum for *h(t)* is higher than that of *f(t)*. This limitation is critical, for we need to have

$$H[a(t)\cos\theta(t)] = a(t)\,H[\cos\theta(t)]; \tag{1.19}$$

otherwise, we cannot use Equation 1.5 to define the phase function. According to the Bedrosian theorem, Equation 1.19 is true only if the amplitude is varying so

slowly that the frequency spectra of the envelope and the carrier waves are disjoint. This has made the application of the Hilbert transform even to IMFs problematic. To satisfy this requirement, Huang and Long (2003) have proposed the normalization of the IMFs in the following steps: starting from an IMF, we first find all the maxima of the IMFs, defining the envelope by spline through all the maxima and designating the envelope as *E(t)*. Now, we normalize the IMF by dividing the IMF by *E(t)*. Thus, we have the normalized function with amplitude always equal to unity.

Even with this normalization, we have not resolved all the limitations on the Hilbert transform. The new restriction is given by the Nuttall theorem (1966). This theorem states that the Hilbert transform of cosine is not necessarily the sine with the same phase function for a cosine with an arbitrary phase function. Nuttall gave an error bound, ΔE, defined as the difference between *y(t)*, the Hilbert transform of the data, and *Q(t)*, the quadrature (with phase shift of exactly 90°) of the function:

$$\Delta E = \int_{t=0}^{T} \left| y(t) - Q(t) \right|^2 dt = \int_{-\infty}^{0} S_q(\omega)\, d\omega \ , \tag{1.20}$$

where S_q is Fourier spectrum of the quadrature function. The proof of this theorem is rigorous, but the result is hardly useful, for it gives a constant error bound over the whole data range. For a nonstationary time series, such a constant bound will not reveal the location of the error on the time axis.

With the normalized IMF, Huang and Long (2003) have proposed a variable error bound based on a simple argument, which goes as follows: let us compute the difference between the squared amplitude of the normalized IMF and unity. If the Hilbert transform is exactly the quadrature, then the squared amplitude of the normalized IMF should be unity; therefore, the difference between it and unity should be zero. If the squared amplitude is not exactly unity, then the Hilbert transform cannot be exactly the quadrature. Consequently, the error can be measured simply by the difference between the squared normalized IMF and unity, which is a function of time. Huang and Long (2003) and Huang et al. (2005) have conducted detailed comparisons and found the result quite satisfactory.

Even with the error indicator, we can only know that the Hilbert transform is not exactly the quadrature; we still do not have the correct answer. This prompts the suggestion of a drastic alternative, eschewing the Hilbert transform totally. To this end, Huang et al. (2005) suggest that the phase function can be found by computing the arc-cosine of the normalized function. A checking of the results so obtained has also proved to be satisfactory. The only problem is that the imperfect normalization will give some values greater than unity. Under that condition, the arc-cosine will break down.

An example of the normalized and regular Hilbert transforms is given in Figure 1.14, from the data given in Figure 1.12c. There are three different instantaneous frequency values: the instantaneous frequency from regular Hilbert transform, the normalized Hilbert transform, and the generalized zero-crossing, which can serve as the standard in the mean. It is easy to see that the normalized instantaneous

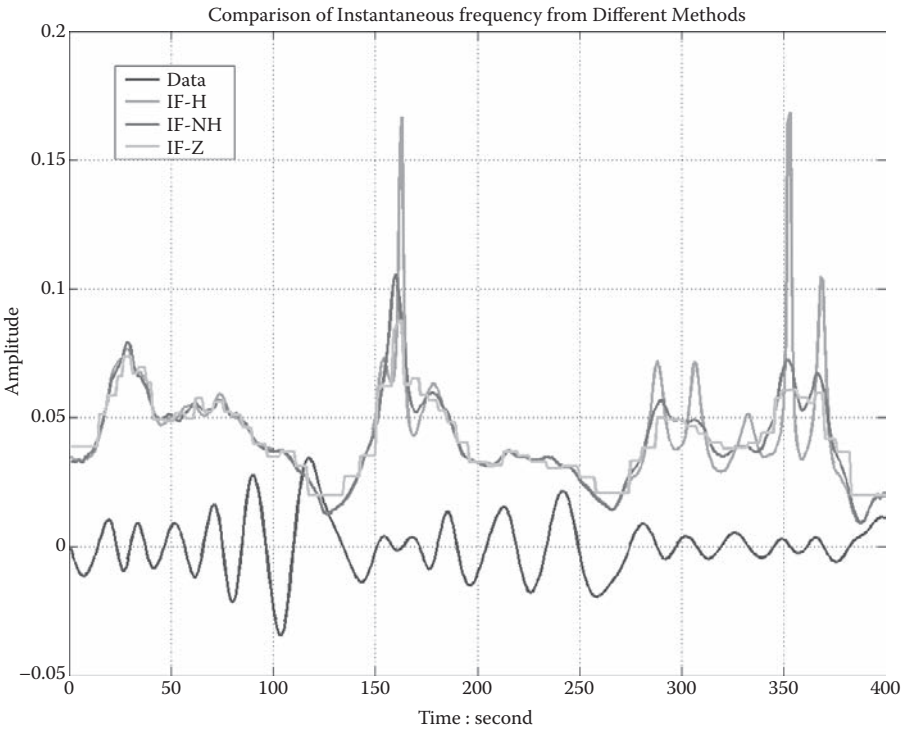

FIGURE 1.14 (See color insert following page 20). Comparison of the instantaneous frequency values derived from different methods. Note that the Instantaneous from IMF is still not correct when the amplitude fluctuates too much. The normalized Hilbert Transform, however, gives a much better instantaneous frequency when compared with the values derived from the generalized-zero-crossing method.

frequency is very close to the zero-crossing values, while the regular Hilbert transform result gives large undulations that will never result in the mean as given by the zero-crossing method. The high undulation results from the large changes of amplitude and some nonlinear distortions of the waveform, both of which will cause the envelope to fluctuate as shown in Figure 1.15. In the normalization scheme, the smooth spline helps to eliminate many of the undulations in the resulting instantaneous frequency. One can also see that the problem of the regular Hilbert transform occurs always at the location where either the amplitudes change drastically or the amplitude is very low, as predicted by the Nuttall theorem. The normalized Hilbert transform alleviates the problems substantially.

Finally, the error index is given in Figure 1.16; here we can see that the error is also small in general, unless the waveform is locally distorted. Even over the large error location, the index values are smaller than 10%, except for the end region, where the end effect of the Hilbert transform causes additional problems. Thus the normalized Hilbert transform has helped to overcome many of the difficulties of the regular Hilbert transform, and it should be used all the time.

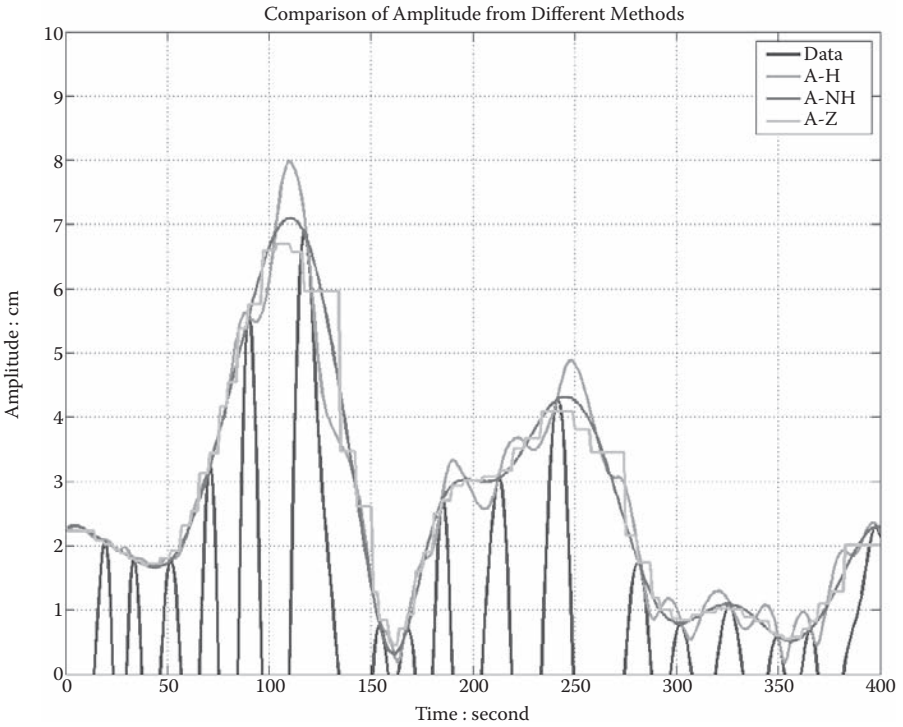

FIGURE 1.15 (See color insert following page 20). The instantaneous amplitude (or the envelope) of the test data. Note the improvement in adopting the spline envelope over the simple analytic function.

1.3.2 The Confidence Limit

The confidence limit for the Fourier spectral analysis is routinely computed. The computation, however, is based on the practice of cutting the data into N sections and computing spectra from each section. The confidence limit is defined as the statistical spread of the N different spectra. This practice is based on the ergodic theory, where the temporal average is treated as the ensemble average. The ergodic condition is satisfied only if the processes are stationary; otherwise, averaging them will not make sense. Huang et al. (2003) have proposed a different approach, using the fact that there are infinitely many ways to decompose one given function into different components. Even using EMD, we can still obtain many different sets of IMFs by changing the stoppage criteria. For example, Huang et al. (2003) explored the stoppage criterion by changing the *S*-number. Using the length-of-day (LOD) data, they varied the *S*-number from 1 to 20 and found the mean and the standard deviation for the Hilbert spectrum given in Figure 1.15. The confidence limit so derived does not depend on the ergodic theory. By using the same data length, there is also no downgrading of the spectral resolution in frequency space through subdividing of the data into sections.

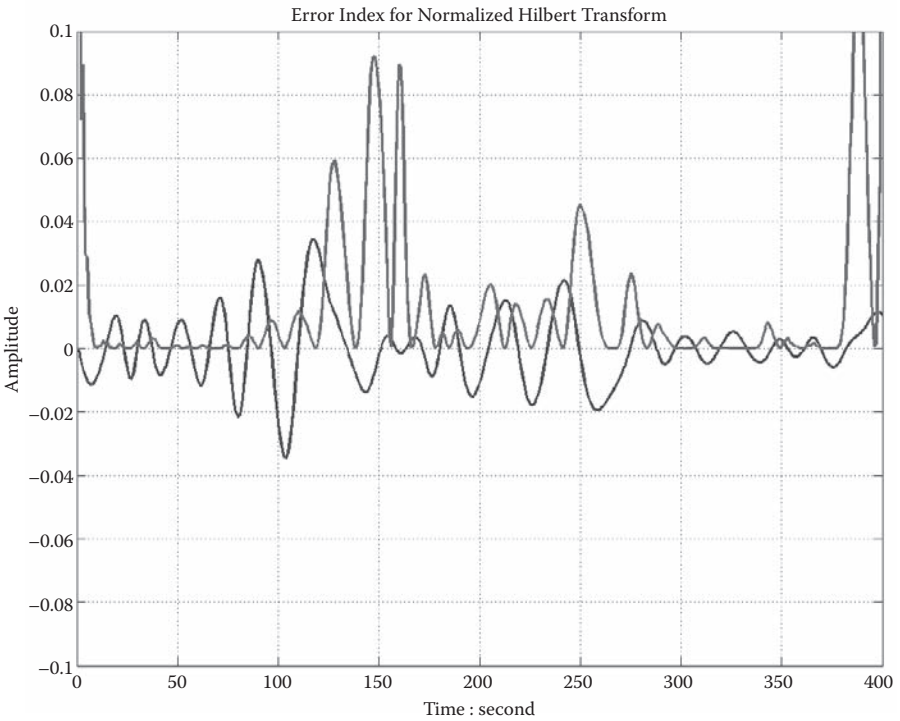

FIGURE 1.16 (See color insert following page 20). The Error Index of the normalized Hilbert transform; it has large value whenever the wave form deviated from a smooth sinusoidal form. But their values are, in general, small except near the ends.

Additionally, Huang et al. (2003) invoked the intermittence criterion and forced the number of IMFs to be the same for different *S*-numbers. As a result, they were able to find the mean for specific IMFs. Figure 1.17 shows the IMF representing variations of the annual cycle of the length of day. The peak and valley of the envelope represent the El Niño events. Of particular interest are the periods of high standard deviations, from 1965 to 1970 and from 1990 to 1995. These periods turn out to be the anomaly periods of the El Niño phenomena, when the sea surface temperature readings in the equatorial region were consistently high based on observations, indicating a prolonged heating of the ocean, rather than the changes from warm to cool during the El Niño to La Niña changes.

Finally, from the confidence limit study, an unexpected result was the determination of the optimal *S*-number. Huang et al. (2003) computed the difference between the individual cases and the overall mean and found that there is always a range where the differences reach a local minimum. Based on their limited experience from different data sets, they concluded that an *S*-number in the range of 4 to 8 performed well. Logic also dictates that the *S*-number should not be too high (which would drain all the physical meaning out of the IMF) nor too low (which would leave some riding waves remaining in the resulting IMFs).

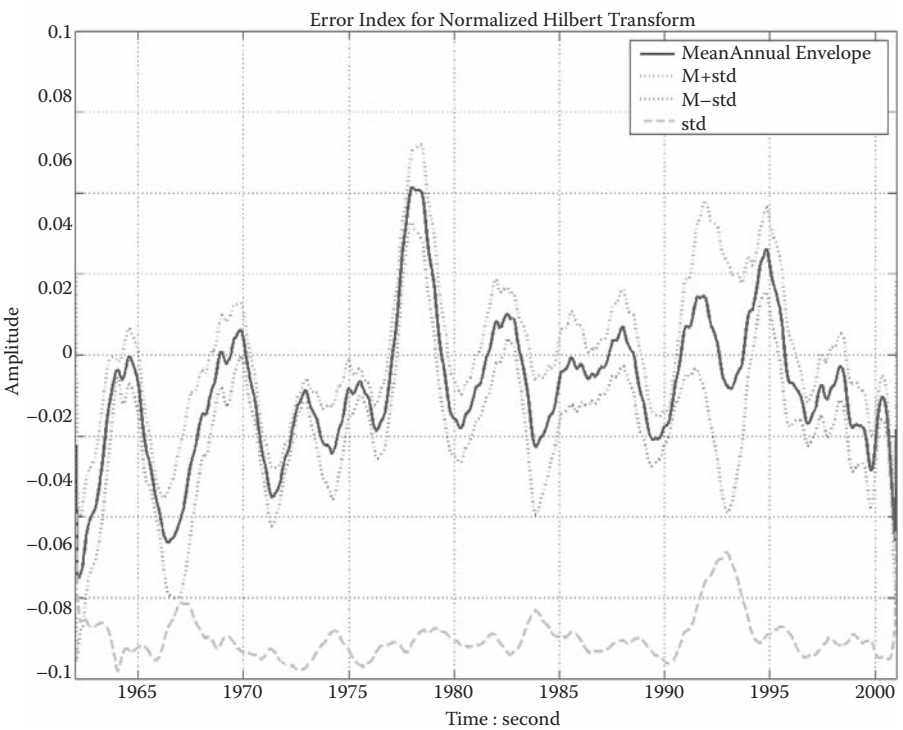

FIGURE 1.17 (See color insert following page 20). The mean envelope of the annual cycle IMF component from LOD data. The peaks of the envelope are all aligned with El Nio events, when the additional angular momentum imparted to the atmosphere from the over heated Equatorial ocean water. The large scatter of the envelope periods in 1065-70 and 1990-95 represent periods of El Nio anomalies.

1.3.3 The Statistical Significance of IMFs

The EMD is a method of separating data into different components by their scales. There is always the question: on what is the statistical significance of the IMFs based? In data that contains noise, how can we separate the noise from information with confidence? This question was addressed by both Flandrin et al. (2004) and Wu and Huang (2004) through the study of signals consisting of noise only.

Flandrin et al. (2004) studied the fractal Gaussian noises and found that the EMD is a dyadic filter. They also found that when one plotted the mean period and root-mean-square (RMS) values of the IMFs derived from the fractal Gaussian noise on log–log scale, the results formed a straight line. The slope of the straight line for white noise is –1; however, the values change regularly with the different Hurst indices. Based on these results, Flandrin et al. (2004) suggested that the EMD results could be used to discriminate what kind of noise one was encountering.

Instead of fractal Gaussian noise, Wu and Huang (2004) studied the Gaussian white noise only. They also found the relationship between the mean period and RMS values of the IMFs. Additionally, they have also studied the statistical properties of the scattering of the data and found the bounds of the data distribution analytically. From the scattering, they deduced a 95% bound for the white noise. Therefore, they concluded that when a data set is analyzed with EMD, if the mean period-RMS values exist within the noise bounds, the components most likely represent noise. On the other hand, if the mean period-RMS values exceed the noise bounds, then those IMFs must represent statistically significant information.

1.4 CONCLUSION

HHT is a relatively new method in data analysis. Its power is in the totally adaptive approach that it takes, which results in the adaptive basis, the IMFs, from which the instantaneous frequency can be defined. This offers a totally new and valuable view of nonstationary and nonlinear data analysis methods. With the recent developments on the normalized Hilbert transform, the confidence limit, and the statistical significance test for the IMFs, the HHT has become a more robust tool for data analysis, and it is now ready for a wide variety of applications. The development of HHT, however, is not over yet. We still need a more rigorous mathematical foundation for the general adaptive methods for data analysis, and the end effects must be improved as well.

REFERENCES

Bedrosian, E. (1963). On the quadrature approximation to the Hilbert transform of modulated signals. *Proc. IEEE, 51,* 868–869.

Cohen, L. (1995). *Time-Frequency Analysis*. Prentice Hall, Englewood Cliffs, NJ.

Diks, C. (1997). *Nonlinear Time Series Analysis*. World Scientific Press, Singapore.

Daubechies, I. (1992). *Ten Lectures on Wavelets*. SIAM, Philadelphia.

Flandrin, P. (1999). *Time-Frequency/Time-Scale Analysis*. Academic Press, San Diego, CA.

Flandrin, P., Rilling, G., and Gonçalves, P. (2004). Empirical mode decomposition as a filterbank. *IEEE Signal Proc. Lett. 11* (2): 112–114.

Hahn, S. L. (1996). *Hilbert Transforms in Signal Processing*. Artech House, Boston.

Huang, N. E., and Long, S. R. (2003). A generalized zero-crossing for local frequency determination. U.S. Patent pending.

Huang N. E., Long, S. R., and Shen, Z. (1996). Frequency downshift in nonlinear water wave evolution. *Advances in Appl. Mech. 32*, 59–117.

Huang, N. E., Shen, Z., Long, S. R. (1999). A new view of nonlinear water waves — the Hilbert spectrum. *Ann. Rev. Fluid Mech. 31,* 417–457.

Huang, N. E., Shen, Z., Long, S. R., Wu, M. C., Shih, S. H., Zheng, Q., Tung, C. C., and Liu, H. H. (1998). The empirical mode decomposition method and the Hilbert spectrum for non-stationary time series analysis. *Proc. Roy. Soc. London, A454*, 903–995.

Huang, N. E., Wu, Z., Long, S. R., Arnold, K. C., Blank, K., Liu, T. W. (2005). On instantaneous frequency. *Proc. Roy. Soc. London* (submitted).

Huang, N. E., Wu, M. L., Long, S. R., Shen, S. S. P., Qu, W. D., Gloersen, P., and Fan, K. L. (2003). A confidence limit for the empirical mode decomposition and the Hilbert spectral analysis. *Proc. Roy. Soc. London, A459*, 2317–2345.

Kantz, H., and Schreiber, T. (1997). *Nonlinear Time Series Analysis*. Cambridge University Press, Cambridge.

Nuttall, A. H. (1966). On the quadrature approximation to the Hilbert transform of modulated signals. *Proc. IEEE, 54,* 1458–1459.

Priestley, M. B. (1988). *Nonlinear and nonstationary time series analysis*. Academic Press, London.

Tong, H. (1990). *Nonlinear Time Series Analysis*. Oxford University Press, Oxford.

Wu, Z., and Huang, N. E. (2004). A study of the characteristics of white noise using the empirical mode decomposition method. *Proc. Roy. Soc. London, A460,* 1597–1611.

References

1 Chapter 1

Bedrosian, E. (1963). On the quadrature approximation to the Hilbert transform of modulated signals. Proc. IEEE, 51, 868–869.

Cohen, L. (1995). Time-Frequency Analysis. Prentice Hall, Englewood Cliffs, NJ.

Diks, C. (1997). Nonlinear Time Series Analysis. World Scientific Press, Singapore.

Daubechies, I. (1992). Ten Lectures on Wavelets. SIAM, Philadelphia.

Flandrin, P. (1999). Time-Frequency/Time-Scale Analysis. Academic Press, San Diego, CA.

Flandrin, P., Rilling, G., and Gonçalves, P. (2004). Empirical mode decomposition as a filterbank. IEEE Signal Proc. Lett. 11 (2): 112–114.

Hahn, S. L. (1996). Hilbert Transforms in Signal Processing. Artech House, Boston.

Huang, N. E., and Long, S. R. (2003). A generalized zero-crossing for local frequency determination. U.S. Patent pending.

Huang N. E., Long, S. R., and Shen, Z. (1996). Frequency downshift in nonlinear water wave evolution. Advances in Appl. Mech. 32, 59–117.

Huang, N. E., Shen, Z., Long, S. R. (1999). A new view of nonlinear water waves — the Hilbert spectrum. Ann. Rev. Fluid Mech. 31, 417–457.

Huang, N. E., Shen, Z., Long, S. R., Wu, M. C., Shih, S. H., Zheng, Q., Tung, C. C., and Liu, H. H. (1998). The empirical mode decomposition method and the Hilbert spectrum for non-stationary time series analysis. Proc. Roy. Soc. London, A454, 903–995.

Huang, N. E., Wu, Z., Long, S. R., Arnold, K. C., Blank, K., Liu, T. W. (2005). On instantaneous frequency. Proc. Roy. Soc. London (submitted).

Huang, N. E., Wu, M. L., Long, S. R., Shen, S. S. P., Qu,

W. D., Gloersen, P., and Fan, K. L. (2003). A confidence limit for the empirical mode decomposition and the Hilbert spectral analysis. Proc. Roy. Soc. London, A459, 2317–2345.

Kantz, H., and Schreiber, T. (1997). Nonlinear Time Series Analysis. Cambridge University Press, Cambridge.

Nuttall, A. H. (1966). On the quadrature approximation to the Hilbert transform of modulated signals. Proc. IEEE, 54, 1458–1459.

Priestley, M. B. (1988). Nonlinear and nonstationary time series analysis. Academic Press, London.

Tong, H. (1990). Nonlinear Time Series Analysis. Oxford University Press, Oxford.

Wu, Z., and Huang, N. E. (2004). A study of the characteristics of white noise using the empirical mode decomposition method. Proc. Roy. Soc. London, A460, 1597–1611.

9 Chapter 9

APPENDIX: RELATION BETWEEN HILBERT MARGINAL

SPECTRUM AND FOURIER ENERGY SPECTRUM Consider a time series y(t) which allows Fourier transform, defined as follows: (9A.1)

Its complex conjugate is then (9A.2)

Now if we define the Fourier energy spectrum by (9A.3)

then the area under the Fourier energy spectrum for all frequency is given by y y t e dt i t ( ) ( )ω ω = − −∞ ∞ ∫ y y t e dt i t∗ −∞ ∞ = ∫ ( ) ( )ω ω E y f ( ) ( )ω ω= 2 E y y d y t y t e d dt dt i t i t = = ∗ − + ( ) ( ) ( ) ( )ω ω ω ω ω ω 1 2 1 2 1 2 −∞ ∞ −∞ ∞ −∞ ∞ −∞ ∞ ∫∫∫∫ = − −∞ ∞ −∞ ∞ ∫∫ y t y t t t dt dt( ) ( ) ( ) 1 2 1 2 1 2 2πδ (9A.4)

if y(t) is defined for 0 < t < T, and zero otherwise. Therefore, the area under the

Fourier energy spectrum defined by Equation 9A.3 is equal to 2π times the total

energy of the time series, defined by the integral of the square of the time series. The area under the Hilbert energy spectrum can be illustrated by a simple case

of a time series that is a summation of n sine functions defined for a given time

period 0 to T, for 0 < t < T (9A.5)

where T = mπ/2ω j for all j, m an integer. When we apply EMD to y(t), we in effect recover the n sine functions as n

IMFs. From Equation 9.1, Equation 9.2, and Equation 9.3 (in the text), one can see

that if C j (t) = A j sinω j t, the Hilbert transform of each of the sine functions produces

D j (t) = −A j cosω j t, and a j 2 (t) = A j 2 . The Hilbert energy spectrum is therefore equal to

A j 2 at ω j for all time. For a finite period of time T, the discrete marginal spectrum is

equal to A j 2 Tat ω j . The total area under the Hilbert

marginal spectrum is therefore

The total energy over the time period is given by (9A.6)

Hence, the total area under Hilbert marginal spectrum is = 2 (9A.7) More generally, for an arbitrary time series, (9A.8) = = −∞ ∞ ∫ ∫ 2 2 2 2 0 π πy t dt y t dt T ( ) ( ) y t A t j j j n ( ) sin( )= = Σ ω 1 A T j j n 2 1 . = Σ y t dt T Aj T j n 2 0 2 1 1 2 ( ) ∫ Σ = = A T j j n 2 1= Σ y t dt T 2 0 ( ) ∫ y t a t t j j j n ( ) ( ) cos[( )]= · = Σ θ 1

if we neglect the residual term from Equation 9.5. Its total area under the Hilbert

marginal spectrum is

Its total energy over time is (9A.9)

Due to the orthogonality of IMFs (see Huang et al. [22]), the cross-terms (i ≠ j) in

Equation 9A.9 can be neglected. Equation 9A.9 reduces to (9A.10) When the IMFs have relatively smooth and sinusoidal shapes, for integer number

of quarter-waves, we have (9A.11) For high-frequency IMFs, the number of quarter-waves is usually large, so the

portion that does not contain a complete quarter-wave is small and can be neglected.

For low-frequency IMFs, this portion cannot be neglected, but low-frequency IMFs

usually have small amplitudes and contribute insignificantly to the total energy.

Therefore one arrives at (9A.12) The total area under Hilbert marginal spectrum is (9A.13)

which is the same as in Equation 9A.7. a t dt j T j n 2 0 1 ∫ Σ = ( ) . y t dt a t a t t T T i j i j n 2 0 0 1 ( ) ( ) ( )cos[( )]cos[∫ ∫ Σ = = θ θ j i n t dt( )] = Σ 1 y t dt a t t dt T j T j j n 2 0 2 0 2 1 ( ) ( )cos [( )] ∫ ∫ Σ = = θ a t t dt a t dt j j T j T 2 2 0 2 0 1 2 ( )cos [( )] ( )θ ∫ ∫ ≈ y t dt a t dt T j T j n 2 0 2 0 1 1 2 ( ) ( ) ∫ ∫ Σ ≈ = a t dt y t dt j T j n T 2 0 1 2 0 2 ∫ Σ ∫ = ≈( ) ( ) Comparing Equation 9A.13 with Equation 9A.4, we conclude that the total area

under the Hilbert marginal spectrum needs to be multiplied by a factor, to be

comparable with the area under the Fourier energy spectrum defined by Equation

9A.3.

FIGURE 10.20 (continued) (e)

S c

a l e 163 Scale of colors from MIN to MAX

A m

p l

i t u

d e −80 −60 −40 −20 500 1000 1500 2000 2500 3000 3500 4000 4500 5000 0 80 60 40 20 Coefficients Line - Ca, b for scale a = 163 (frequency = 49.847) Time

10. Huang H, Norden E, Chern C C, Huang K, Salvino L W, Long S R and Fan K L (2001). A New Spectral Representation of Earthquake Data: Hilbert Spectral Analysis of Station TCU129, Chi-Chi, Taiwan, 21 September 1999. Bull. Seism. Soc. Am. 91(5):1310–1338. 11. Zhang R R, King R, Olson L and Xu Y (2001). A HHT View of Structural Damage from Vibration Recordings Proc. ICOSSAR '01 (San Diego) – CD. 12. Shim S H, Jang S A, Lee J J and Yun C B (2002). Damage Detection Method for Bridge Structures Using Hilbert-Huang Transform Technique. 2 nd Int. Conf. Struct. Stab. Dynam., Dec. 16–18, 2002, Singapore. 13. Quek S T, Tua P S and Wang Q (2003). Detecting Anomaly in Beams and Plate Based on Hilbert-Huang Transform of Real Signals. Smart Mater. Struct. 12(3): 447–460. 14. Tua P S, Jin J, Quek S T and Wang Q (2002). Analysis of Lamb Modes Dominance in Plates via Huang Hilbert Transform for Health Monitoring. Proc. 15 KKCNN Symp. Civil Eng., Ed. S T Quek and D W S Ho, Dec. 19–20, 2002, Singapore. 15. Hahn S L (1996). Hilbert Transform in Signal Processing. London: Artech House Boston. 16. Graff K F (1975). Wave Motion in Elastic Solids. Oxford: Clarendon Press. 17. Huang H, Norden E, Zheng S and Long S R (1999). A New View of Nonlinear Water Waves: The Hilbert spectrum. Annu. Rev. Fluid Mech. 31:417–457.

11 Chapter 11

FIGURE 11.15 YPGDV ψ 2 data. Top: Signal and residual (dotted line). Middle: Signal after

the residual is removed (equivalent to the sum of the IMFs). Bottom: IMFs generated by EMD. 8. Zhang, X., Wozniak, J. A., Matthews, B. W. (1995). Protein flexibility and adaptability seen in 25 crystal forms of T4 lysozyme. J. Mol. Biol. 250:527–522. 9. Hayward, S. (1999). Structural principles governing domain motions in proteins. Proteins: Struct. Funct. Genet. 36:425–435. 10. Gogo, N. K., Skrynnikov, N. R., Dahlquist, F. W., Kay, L. E. (2001). What is the average conformation of bacteriophage T4 lysozyme in solution? A domain orientation study using dipolar couplings measured by solution NMR. J. Mol. Biol. 308: 745–764. 11. Amadei, A., Linssen, A. B. M., Berendsen, H. J. C. (1993). Essential dynamics of proteins. Proteins: Struct. Funct. Genet. 17(4):412–425. 12. Buchner, M., Ladanyi, B. M., Stratt, R. M. (1992). The short-time dynamics of molecular liquids. Instantaneous-normal-mode theory. J. Chem. Phys. 97(11):8522– 8535. 13. de Groot, B. L., Hayward, S., van Aalten, D. M. F., Amadei, A., Berendsen, H. J. C. (1998). Domain motions in bacteriophage T4 lysozyme: a comparison between molecular dynamics and crystallographic data. Proteins: Struct. Funct. Genet. 31: 116–127. 14. Sanders, J. K. M., Hunter, B. K. (1993). Modern NMR Spectroscopy. 2nd ed. Oxford: Oxford University Press. 15. Johnson, W. C. (1990). Protein secondary structure and circular dichroism — a practical guide. Proteins: Struct. Funct. Genet. 7(3):205–214. 16. Fischer, M. W. F., Majumdar, A., Dahlquist, F. W., Zuiderweg, E. R. P. (1995). 15 N, 13 C, and 1 H NMR assignments and secondary structure for T4-lysozyme. J. Magn. Reson., Ser. B 108:143–154 17. Mulder, F. A. A., Mittermaier, A., Hon, B., Dahlquist, F. W., Kay, L. E. (2001). Studying excited states of proteins by NMR spectroscopy. Nat. Struct. Biol. 8(11): 932–935. 18. Scott, W. R. P., Schiffer, C. A. (2000). Curling of flap tips in HIV1 protease as a mechanism for substrate entry and tolerance of drug resistance. Structure 8: 1259–1265. 19. Verlet, L. (1967). Computer experiments on classical fluids. I. Thermodynamical properties of Lennard-Jones molecules. Phys. Rev. 159:98–103. 20. Weiner, P.W., Kollman, P.A. (1981). AMBER: assisted model building with energy refinement. A general program for modelling molecules and their interactions. J. Comput. Chem., 4:287–303. 21. Woodcock, L. V. (1971). Isothermal molecular dynamics calculations for liquid salts. Chem. Phys. Lett. 10:257–261. 22. Berendsen, H. J. C., Postma, J. P. M., van

Gunsteren, W. F., Di Nola, A., Haak, J. R. (1984). Molecular dynamics with coupling to an external bath. J. Chem. Phys. 81: 3684-3690. 23. Anderson, H. C. (1980). Molecular dynamics simulations at constant pressure and/or temperature. J. Chem. Phys. 72:2384-2393. 24. Hoover, W. G. (1985). Canonical dynamics: equilibrium phase-space distributions. Phys. Rev. A31:1695-1697. 25. Creighton, T. E. (1993). Conformational properties of polypeptide chains. In: Proteins structures and molecular properties. 2nd ed. New York: W. H. Freeman and Company, pp. 192-193. 26. Sessions, R. B., Dauber-Osguthorpe, P., Osguthorpe, D. J. (1989). Filtering moleculardynamics trajectories to reveal low-frequency collective motions — phospholipaseA2. J. Mol. Biol. 210(3):617-633. 27. Levitt, M. (1991). Real-time interactive frequency filtering of moleculardynamics trajectories. J. Mol. Biol. 220(1):1-4. 28. Phillips, S. C., Essex, J. W., Edge, C. M. (2000). Digitally filtered molecular dynamics: the frequency specific control of molecular dynamics simulations. J. Chem. Phys. 112(6):2586-2597. 29. Phillips, S. C., Swain, M. T., Wiley, A. P., Essex, J. W., Edge, C. M. (2003). Reversible digitally filtered molecule dynamics. J. Phys. Chem. B. 107(9):2098-2110. 30. Phillips, S. C., Gledhill, R. J., Essex, J. W., Edge, C. M. (2003). Application of the Hilbert-Huang transform to the analysis of molecular dynamics simulations. J. Phys. Chem. A. 107(24):4869-4876. 31. Huang, N. E., Chen, Z., Long, S. R., Wu, M. L. C., Shih, H. H., Zheng, Q. N., Yen, N. C., Tung, C. C., Liu, H. H. (1971). The empirical mode decomposition and the Hilbert spectrum for nonlinear and nonstationary time series analysis. Proc. R. Soc. London Ser. A Math. Phys. Eng. Sci. 454:903-995. 32. Echeverria, J. C., Crowe, J. A., Woolfson, M. S., HayesGill, B. R. (2001). Application of empirical mode decomposition to heart rate variability analysis. Med. Biol. Eng. Comput. 39(4):471-479. 33. Chen, K. Y., Yeh, H. C., Su, S. Y., Liu, C. H., Huang, N. E. (2001). Anatomy of plasma structures in an equatorial spread F event. Geophys. Res. Lett. 28(16): 3107-3110. 34. Komm, R. W., Hill, F., Howe, R. (2001). Empirical mode decomposition and Hilbert analysis applied to rotation residuals of the solar convection zone. Astrophys. J. 558(1):428-441. 35. Bendat, J. S. (1985). The Hilbert transform and application to correlation measurements. Denmark: Brüel & Kjær. 36. Wu, X. W., Wang, S. M. (2000). Folding studies of a linear pentamer peptide adopting a reverse turn conformation in aqueous solution through molecular dynamics simulations. J. Phys. Chem. B. 104(33):8023-8034. 37. Dyson, H. J., Rance, M., Houghten, R. A., Wright, P. E., Lerner, R. A. (1988). Folding of immunogenic peptide-fragments of proteins in water solution. 2. The nascent helix. J. Mol. Biol.

201(1):201–217. 38. MATLAB 5.3.0. Natick, MA: The MathWorks Inc. (1999). 39. Swope, W. C., Andersen, H. C., Berens, P. H., Wilson, K. R. (1982). A computersimulation method for the calculation of equilibrium-constants for the formation of physical clusters of molecules — application to small water clusters. J. Chem. Phys. 76(1):637–649.

12 Chapter 12

Chan, Y.T. (1995). Wavelet basics. Boston: Kluwer.

Deng, Y.J., W. Wang, C.C. Qian, Z. Wang and D.J. Dai. (2001). Boundary-processing technique in EMD method and Hilbert transform. Chinese Science Bulletin, 46(11), 954–960.

Huang, N.E., Z. Shen, S.R. Long, et al. (1998). The empirical mode decomposition and the Hilbert spectrum for nonlinear and non-stationary time series analysis. Proc. R. Soc. Lond. A, 454, 899–995.

Huang, N.E., Z. Shen and S.R. Long. (1999). A new view of nonlinear water waves: the Hilbert spectrum. Annu. Rev. Fluid Mech., 31, 417–457.

13 Chapter 13

Attoh-Okine, N. O. (1999). Application of Wavelets in Pavement Profile Evaluation and Assessment. Proc. Estonian Acad. Science, 5, 53–63.

Attoh-Okine, N. O. (2004). Comparative Analysis of Hilbert-Huang Transform and Maximal Overlap Discrete Wavelet Packet Transform. Working paper, University of Delaware Engineering Department.

Chen, C. H., Li, C. P., and Teng, T. L. (2002a). Surface-Wave Dispersion Measurements Using Hilbert-Huang Transform. TAO 13, 2:171–184.

Chen, J., and Xu, Y. L. (2002). Identification of Modal Damping Ratios of Structures with Closely Spaced Modal Frequencies. Struct. Eng. Mech. 14, 4:417–434.

Chen, Y., and Feng, M. Q. (Undated). A Technique to Improve the Empirical Mode of Decomposition in the Hilbert-Huang Transform. p. 24.

Chun-xiang, S., and Qi-feng, L. (2003). Hilbert-Huang Transform and Wavelet Analysis of Time History Signal. Acta Seismological Sinica 166, 4:422–429.

Datig, M., and Schlurmann, T. (2004). Performance and Limitation of the Hilbert Huang Transformation with an Application to Irregular Water Waves. Ocean Eng. 31, 14–15: 1783–1834.

Deng, Y., et al. (2001). Boundary-Processing Technique in EMD Method and Hilbert Transform. Chinese Science Bull. 46, 11:954–961.

Duffy, D. (2004). The Application of Hilbert Huang Transform to Meteorological Datasets. J. Atmospheric Oceanic Technol. 21, 599–611.

Flandrin, P., Rilling, G., and Goncalves, P. (2003). Empirical Mode of Decomposition as a Filter Bank. IEEE Signal Process. Lett.

Gabor, D. (1946). Theory of Communication. Proc. IEE 93, 429–457.

Gu, P., and Wen, Y. K. (2005). Simulation of Nonstationary Random Processes Using Instantaneous Frequency and Amplitude from Hilbert Huang Transform. In this Volume.

Huang, N. E., et al. (1999a). A New View of Nonlinear Water Waves: The Hilbert Spectrum. Annu. Rev. Fluid Mech. 31, 417-57.

Huang N. E., et al. (2003a). A Confidence Limit for the Empirical Mode Decomposition and Hilbert Spectrum Analysis. Proc. R. Soc. London A, 459, 2317-2344.

Huang, N. E., Chern, C. C., Huang, K., Salvino, L. W., Long, S. R., and Fan, K. L. (2001). A New Spectral Representation of Earthquake Data: Hilbert Spectral Analysis of Station TCU129, Chi-Chi Taiwan, 21 September 1999. Bull. Seismological Soc. Am. 91, 5:1310-1338.

Huang, N. E., Shen, Z., Long, S. R., Wu, M. C., Shih, E. H., Zheng, Q., Tung, C. C., and Liu, H. H. (1998). The Empirical Mode Decomposition Method and the Hilbert Spectrum for Non-Stationary Time Series Analysis. Proc. R. Soc. London A 454, 903-995.

Huang, W., Shen, Z., Huang N. E., and Fung, Y. C. (1999b). Engineering Analysis of Biological Variables: An Example of Blood Pressure Over 1 Day. Proc. National Acad. Science 95, 4816-4821.

Huang, W., Shen, Z., Huang N. E. and Fung, Y. C. (1999c). Nonlinear Indicial Response of Complex Nonstationary Oscillations as Pulmonary Hypertension Responding to Step Hypoxia. Proc. National Acad. Science 96, 1834-1839.

Huang, N. E., Wu, M.-L., Qu, W., Long, S. R., Shen, S. S. P., and Zhang, J. E. (2003b). Application of Hilbert-Huang Transform to Non-Stationary Financial Time Series Analysis. Appl. Stochastic Models Bus. Industry 19, 245-268.

Hwang, P. A., Wang, D. W., and Kaihatu, J. M. (2005). A Comparison of the Energy Flux Computation of Shoaling Waves Using Hilbert and Wavelet Spectral Anlysis Techniques. In this Volume.

Lai, Y. (1998). Analytic Signals and the Transition to Chaos Deterministic Flows. Phys. Rev. E 58, 6:R6911-6914.

Larsen, M. L., Ridgway, J., Waldman, C. H., Gabbay, M., Buntzen, R. R., and Battista, B. (2005). Nonlinear Signal Processing of Underwater Electromagnetic Data. In this Volume.

Li, Y. F., Chang, S. Y., Tzeng, W. C., and Huang, K.

(2003). The Pseudo Dynamic Test of RC Bridge Columns Analyzed Through the Hilbert-Huang Transform. Chin. J. Mech. A 19, 3: 373–387.

Loh, C.-H., Wu, T. C., and Huang, N. E. (2001). Application of the EMD-Hilbert Spectrum to Identify Near-Fault Ground Motion Characteristics and Structural Responses. Bull. Seismological Soc. Am. 191, 5: 1339–1353.

Long, S. R., Huang, N. E., Tung, C. C., Wu, M. L., Lin, R. Q., et al. (1995). The Hilbert Techniques: An Alternative Approach for Non-Steady Time Series Analysis. IEEE Geoscience Remote Sensing Soc. Lett. 3, 3–11.

Lundquist, J. K. (2003). Intermittent and Elliptical Inertia Oscillation in Atmospheric Boundary Layer. J. Am. Meteorological Soc. 60, 2261–2273.

Magrin-Chagnolleau, I., and Baraniuk, R. G. (undated). Empirical Mode Decomposition Based Time Frequency Attribute. pp 4.

Montesinos, M. E., Munoz-Cobo, J. L., and Perez, C. (2002). Hilbert-Huang Analysis of BWR Neutron Detector Signals: Application to DR Calculation and to Corrupted Signal Analysis. Ann. Nuclear Energy 30, 715–727.

Neithammer, M., et al. (2001). Time-Frequency Representations of Lamb Waves. J. Acoustical Soc. Am. 109, 5: Pt. 1, 1841–1847.

Olhede, S., and Walden, A. T. (2004). The Hilbert Spectrum via Wavelet Projections. Proc. R. Society A 460, 2044: 955–975.

Osegueda, R., Kreinovich, V., Nazarian, S., and Roldan, E. (2003). Detection of Cracks at Rivet Holes in Thin Plates Using Lamb-Wave Scanning. Proc. SPIE 5047, 55–66.

Pan, J., Yan, X. H., Zheng, Q., Liu, W. T., and Klemas, V. V. (2002). Interpretation of Scatterometer Ocean Surface Wind Vector EOFs over the Northwestern Pacific. Remote Sensing Environ. 84, 53–68.

Phillips, S. C., Gledhill, R. J., and Essex, J. W. (2003). Applications of the Hilbert-Huang Transform to the Analysis of Molecular Dynamics Simulations. J. Phys. Chem. A 107, 4869–4876.

Pines, D., and Salvino, L. (2002). Health Monitoring of

One-Dimensional Structures Using Empirical Mode Decomposition and the Hilbert-Huang Transform. Proc. SPIE 4701, 127–143.

Qu, J., and Jarzynski, J. (2001). Time Frequency Representation of Lamb Waves. J. Acoust. Soc. Am., 109(5) Part 1, 1841–1847.

Quek, S. T., Tua, P. S., and Wang, Q. (2003). Detecting Anomalies in Beams and Plate Based on the Hilbert- Huang Transform of Real Signals. Smart Mater. Structures 12, 447–460.

Quek, S. T., Tua, P. S., and Wang, Q. (2004). Comparison of Hilbert-Huang, Wavelet, and Fourier Transforms for Selected Applications. In this Volume.

Salisbury, J. I., and Wimbush, M. (2002). Using Modern Time Series Analysis Techniques to Predict ENSO Events from SOI Time Series. Nonlinear Processes in Geophysics 9, 341–345.

Schlurmann, T. (2002). Spectral Analysis of Nonlinear Water Waves Based on the Hilbert-Huang Transformation. Trans. ASME 124, 22–27.

Schlurmann, T., and Datig, M. (2005). Carrier and Riding Wave Structure of Rogue Waves. In this Volume.

Shen, J. J., Yen, W. P., and Fallon, J. O. (2003). Interpretation and Application of Hilbert-Huang Transformation for Seismic Performance Analyses. Advanced Mitigation Technologies 657–666.

Veltcheva, A. (2005). An Application of HHT Method to the Nearshore Sea Waves. In this Volume.

Veltcheva, A. D. (2002). Wave and Group Transformation by a Hilbert Spectrum. Coastal Eng. J. 44, 4: 283–300.

Wang, W. (2005). Decomposition of Wave Groups with EMD Method. In this Volume.

Wen, Y. K., and Gu, P. (2004). Description and Simulation of Nonstationary Processes Based in Hilbert Spectra. J. of Eng. Mech. 130, 8: 942–951.

Wiley, A. P., Gledhill, R. J., Phillips, S. C., Swain, M. T., Edge, C. M., and Essex, J. W. (2005). The Analysis of Molecular Dynamics Simulations by the Hilbert-Huang Transform. In this Volume.

Xiang, S. C., and Feng, L. Q. (2003). Hilbert-Huang Transform and Wavelet Analysis of Time History Signal. Acta Seismological Sinica 16, 4: 422-429.

Xu, Y. L., Chen, S. W., and Zhang, R. C. (2003). Modal Identification of Di Wang Building Under Typhoon York Using the Hilbert-Huang Transform Method. The Structural Design of Tall and Special Buildings 12, 21-47.

Yang, J. N., Lei, Y., Pan, S., and Huang, N. (2003a). System Identification of Linear Structures Based on Hilbert-Huang Spectral Analysis. Part 1: Normal Modes. Earthquake Eng. Structural Dynamics 32: 1443-1467.

Yang, J. N., Lei, Y., Pan, S., and Huang, N. (2003b). System Identification of Linear Structures Based on Hilbert-Huang Spectral Analysis. Part 1: Complex Mode. Earthquake Eng. Structural Dynamics 32: 1533-1554.

Yang, J. N., Lei, Y., Lin, S., and Huang, N. (2004). Hilbert-Huang Based Approach for Structural Damage Detection. J. Eng. Mech. 130, 1: 85-95.

Yang, J. N., Lin, S., and Pan, S. (2002). Damage Identification of Structures Using Hilbert-Huang Spectral Analysis. 15th ASCE Eng. Mech. Conf., New York.

Yu, D., Cheng, J., and Yang, Y. (2003). Application of EMD Method and Hilbert Spectrum to the Fault Diagnosis of Roller Bearings. Mechanical Syst. Signal Process. 19, 2: 259-270.

Zeris, A., and Prinos, P. (2005). Coherent Structures Analysis in Turbulent Open-Channel Flow Using Huang-Hilbert and Wavelets Transforms. In this Volume.

Zhang., R. R. (2004). An HHT Based Approach to Quantify Nonlinear Soil Amplification. In this Volume.

Zhang, R. R., Demark, L. V., Liang, J., and Hu, Y. (2004). On Estimating Site Damping with Soil Non-Linearity from Earthquake Recordings. Int. J. Non-Linear Mech. 39, 1501-1517.

Zhang, R. R., Ma, S., Safak, E., and Hartzell, S. (2003). Hilbert-Huang Transform Analysis of Dynamic and Earthquake Motion Recordings. J. Eng. Mech. 129, 8: 861-875.

ADDENDUM: PERSPECTIVES ON THE THEORY AND PRACTICES

OF THE HILBERT-HUANG TRANSFORM

Recently there have been innovative applications and major improvement to EMD

HHT. These improvements have spread to general analytical approaches, hybrid

applications, and bidimensional HHT.

13A.1 ANALYTICAL

Coughlin and Tung [2004] used EMD to extract the solar cycle signal from strato

spheric data. The authors highlighted some difficulties in using EMD — especially

the influence of the end point in the sifting process. They addressed a method of

reducing the influence of the end effects on the internal solution. Coughlin and Tung

[2004] extended both the beginning and end of the spline by introducing a wave

equation of the form: (13A.1)

The typical amplitude, A, and period p, are determined by the nearest local extrema. (13A.2)

where max(1) and min(1) are the first two local extrema in the time series and

max(N) and min(N) are the last two local extrema. This approach reduces the large

swings in the spline calculation. This approach is quite different from the one

proposed by Dätig and Schlurmman [2004].

13A.2 HYBRID METHOD

Iyengar and Kanth [2004] used HHT to decompose India monsoon data. The authors

argued that the first IMF is nonlinear and the remaining

IMFs are linear. This is a

little questionable, since it is not clear how the authors determined these properties.

The authors used a neural network to forecast the nonlinear part of the data. Lee et

al. [2003] explored the vibration mechanism of a bridge at both global and local

behavior. They proposed a combination of EMD, HHT, and a nonlinear parametric

model as an identification methodology. The approach was successful in identifying

abnormal signals indicating the structural condition of the bridge decks based on

the time-frequency spectrum. Wave Extension = + phase + local mA t p sin 2π ean ⎡ ⎣ | ⎤ ⎦ | A A N N p beginning end = ( ) − ( ) = ( ) − ( ) max min max min 1 1 beginning end time time ti = ( ) − ( ) = 2 1 1 2 max min p me time max minN N ( ) − ( ) Loutridis [2004] used EMD to decompose vibration signals from gear systems.

The author developed an empirical law that relates the energy of the intrinsic modes

to the crack magnitude of the gear. Using this technique, the degree of crack can be

predicted based on energy obtained from the IMFs.

13A.3 BIDIMENSIONAL EMD

Nunes and coworkers developed a method for analyzing two-dimensional (2D) time

series which was used for textural analysis [2003a]. The bidimensional sifting

process they presented in an earlier paper [Nunes et al., 2003] is as follows: • Identify the extrema of the image I by morphological reconstruction based on geodesic operators. • Generate the 2D “envelope” by connecting the maxima points with a radial basis function (RBF). • Determine the local mean m_{ i }, by averaging the two envelopes. • Subtract I − m_{ i } = h_{ i } • Repeat the

process. The authors used a radial basis function in the form: (13A.3)

radial basis function (RBF);

p m is mth degree polynomial in d variables;

λ are RBF coefficients;

x i are the RBF centers. The stopping criteria for Nunes et al. [2003] approach is based on similar to 1D

case used, using the standard deviation. Linderhed [2002] developed a 2D EMD and presented a coding scheme for

image compression purposes. In the coding scheme, only the maximum and mini

mum values of the IMFs are used. Linderhed [2004] also developed the concept of

empiquency, short for empirical mode frequency as a frequency measure.

Empiquency is defined as one half the reciprocal distance between two consecutive

extrema points. Linderhed [2004] developed a sifting process for 2D time series.

The symmetry criterion on the IMF envelope is relaxed, and the stop criterion is

based on the condition that the IMF envelope is close to zero. Hence, there is no

need to check for symmetry. The new sifting process is as follows: 1. Find the positions and amplitudes of all local maxima and minima in the input signal in_{ lk }(m,n), where m and n denote spatial dimensions of the image. 2. Create upper and lower envelopes by spline interpolation, denoted by e_{ max }(m,n) and e_{ min }(m,n). s x p x x x m i i i N ( ) = ( ) + − ( ) = Σ λ Φ 1 3. For each position, calculate the mean of the upper and lower envelopes: (13A.4) 4. Subtract the envelope mean signal from the input signal: (13A.5) The process is terminated if the envelope mean signal is close to zero: (13A.6) for all (m,n). If it is not, the process repeated until: (13A.7) When the termination criterion is achieved, k = K, and the IMF is defined as: (13A.8) 5. The residue is defined as

r_{l}(m,n): (13A.9) 6. The next IMF is found as follows: (13A.10) 7. Just as the 1D series the signal can be represented as: (13A.11) Liu and Peng [2005] proposed a boundary-processing technique for bidimen

sional EMD. The authors proposed two techniques, but unfortunately the two algo

rithms developed by these authors are similar to algorithms proposed by Nunes et

al. [2003] and Linderhead [2004]. em m n e m n e m n lk , , , max min ( ) = ( ) + ( ) 2 h m n in m n em m n lk lk lk , , , ( ) = ( ) − ( ) em m n lk , ( ) ≺ ε h m n h m n l k lk + ( ) ( ) = ( ) 1 , , c m n h m n l lK , , ( ) = ( ) r m n in m n c m n l l l , , , ( ) = ( ) = ( ) 1 in m n r m n l l + ( ) ( ) = ( ) 1 1 , , x m n r m n c m n L j i L , , , ( ) = ( ) + ( ) = Σ 1

13A.4 SOME OBSERVATIONS

The use of bidimensional EMD-HHT is beginning to emerge. Few results indicate

that the 2D HHT outperforms traditional wavelet and Fourier analysis. As with the

1D HHT, there are difficulties regarding the type of spline and the effect of the end

points on the overall sifting process. The use of different RBFs, such as thin plate

splines, cubic spline, and multiquadrics, will be worth exploring in the bidimensional

HHT.

Coughlin, K. T. and Tung, K. K. (2004). 11-Year Solar Cycle in the Stratosphere Extracted by the Empirical Mode Decomposition Method. Adv. Space Res. 34, 323–329.

Dätig, M. and Schlurmann, T. (2004). Performance and Limitations of the Hilbert-Huang Transformation with an Application to Irregular Water Waves. Ocean Eng. 31, 14/15: 1783–1834.

Iyengar, R. N. and Kanth R. S. T. G (2004). Intrinsic Mode Functions and a Strategy for Forecasting Indian Monsoon Rainfall. Meteorol. Atmospheric Phys. (online publication).

Lee, Z. K., Wu, T. H. and Loh, C. H. (2003). System Identification on Seismic Behavior of an Isolated Bridge. Earthquake Eng. Structural Dynamics 32, 1797-1812.

Linderhed, A. (2003). 2-D Empirical Mode Decomposition: In Spirit of Image Compression. SPIE Proc. 4738, 1-8.

Linderhed, A. (2003). Image Compression Based on Empirical Mode Decomposition. Proc. SSBA Symp. Image Anal. 110-113.

Linderhed, A. (2004). Adaptive Image Compression with Wavelet Packets and Empirical Mode Decomposition. Dissertation No. 909 submitted to Linkoping Studies in Science and Technology.

Liu, Z. and Peng, S. (2005). Boundary Processing of Bidimensional EMD Using Texture Synthesis. IEEE Signal Process. Lett. 12, 1: 33-36.

Loutridis, S. J. (2004). Damage Detection in Gear Systems Using Empirical Mode Decomposition. Eng. Structures 26, 1833-1841.

Nunes, J. C., Bouaoune, Y., Delechelle, E., Niang, O. and Bunel P. (2003). Image Analysis by Bidimensional Empirical Mode Decomposition. Image Vision Comput. 21, 1019-1026.

Nunes, J. C., Niang, O., Bouaoune, Y., Delechelle, E., and Bunel P. (2003a). Bidimensional Empirical Mode Decomposition Modified for Texture Analysis. SCIA 2003, Lecture Notes on Computer Science 2749, 171-177.